Biosensors

DOI: 10.1002/anie.200800169

Semiconductor Quantum Dots for Bioanalysis

*Ron Gill, Maya Zayats, and Itamar Willner**

Keywords:
biosensors · nanoparticles · photocurrents · quantum dots · semiconductors

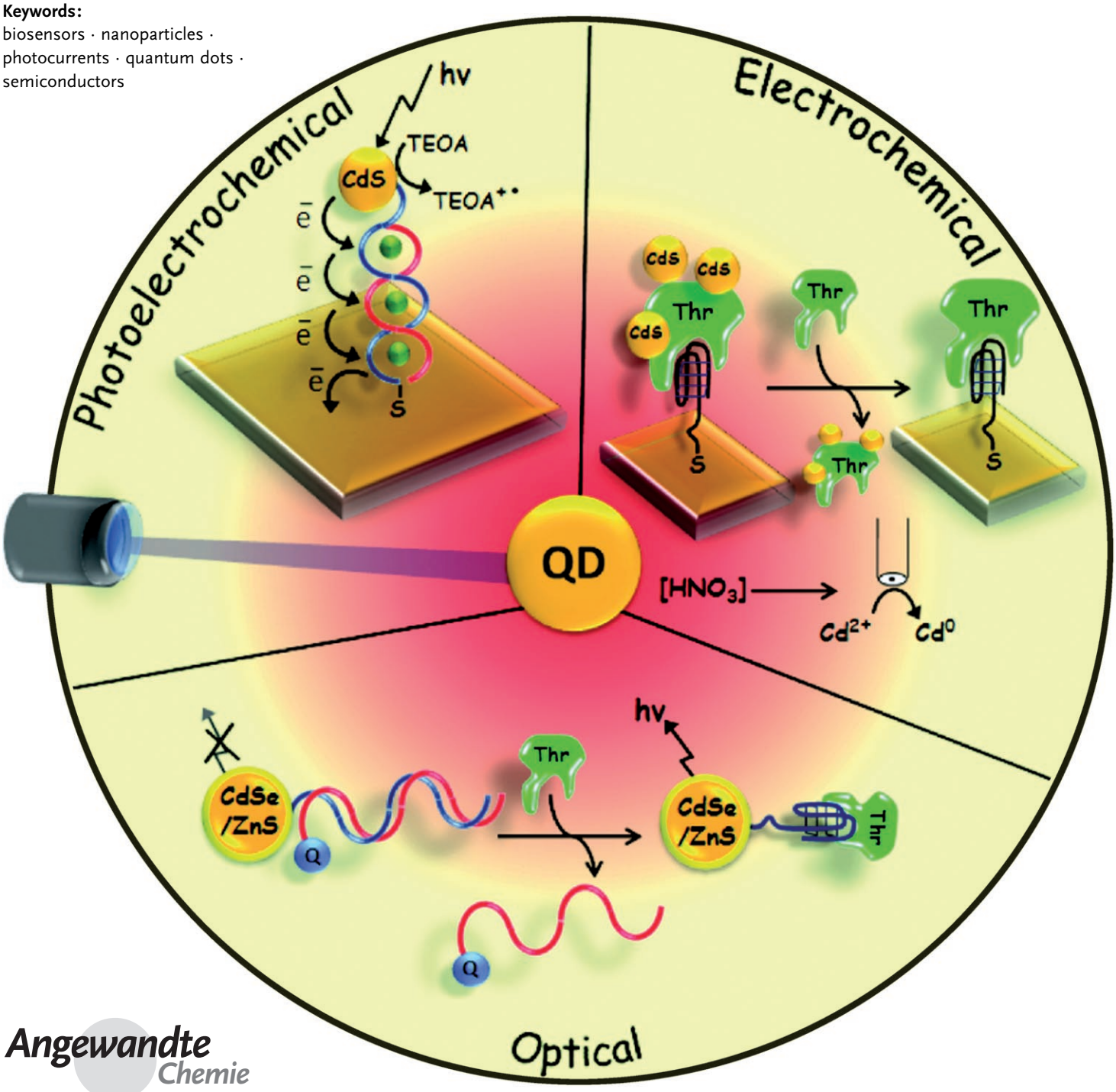

Semiconductor nanoparticles, or quantum dots (QDs), have unique photophysical properties, such as size-controlled fluorescence, have high fluorescence quantum yields, and stability against photobleaching. These properties enable the use of QDs as optical labels for the multiplexed analysis of immunocomplexes or DNA hybridization processes. Semiconductor QDs are also used to probe biocatalytic transformations. The time-dependent replication or telomerization of nucleic acids, the oxidation of phenol derivatives by tyrosinase, or the hydrolytic cleavage of peptides by proteases are probed by using fluorescence resonance energy transfer or photoinduced electron transfer. The photoexcitation of QD–biomolecule hybrids associated with electrodes enables the photoelectrochemical transduction of biorecognition events or biocatalytic transformations. Examples are the generation of photocurrents by duplex DNA assemblies bridging CdS NPs to electrodes, and by the formation of photocurrents as a result of biocatalyzed transformations. Semiconductor nanoparticles are also used as labels for the electrochemical detection of DNA or proteins: Semiconductor NPs functionalized with nucleic acids or proteins bind to biorecognition complexes, and the subsequent dissolution of the NPs allows the voltammetric detection of the related ions, and the tracing of the recognition events.

From the Contents

1. Introduction

Semiconductor nanoparticles (NPs) or quantum dots (QDs) have unique photophysical properties that offer significant advantages as optical labels for biosensing. Typical for semiconductor QDs are high fluorescence quantum yields, stability against photobleaching,[1] and size-controlled luminescence properties.[2–6] The efficient fluorescence and stability of QDs improve sensitivity and prolong lifetime in their use as optical labels. The size-controlled luminescence functions of QDs illustrate the major advantages of QDs as optical labels, as particles of the same material with variable sizes may be used as fluorescent labels for the parallel multiplexed analysis of different analytes. Furthermore, unlike molecular fluorophores which have narrow excitation range, semiconductor QDs have broad absorbance bands. This property allows the excitation of QDs of various sizes at a common wavelength manifold while imaging, in parallel, the fluorescence of the different QDs. Also, effective methods to synthesize semiconductor QDs and to chemically modify the surfaces of the QDs by functional capping monolayers or thin films were developed in recent years.[7] These functional QDs allow the secondary tethering of ligands or receptor units to the surface of the QDs, thus yielding QD–ligand conjugates in which the NP acts as an optical transducer for recognition of sensing events occurring at the surfaces of the NPs.[8,9]

Quantum dots are also photoelectrochemically active.[10] Photoexcitation of the semiconductor QDs results in the transfer of electrons from the valence band to the conduction band, thus yielding electron–hole pairs. Whereas the luminescence properties of QDs originate from radiative electron–hole recombination, trapping of conduction-band electrons in surface traps yields sufficiently long-lived electron–hole pairs to permit the ejection of the trapped electrons to electrodes (or a solution-solubilized electron acceptor A) giving rise to the photoelectrochemical current. The ejection of the conduction-band electrons to the electrode, with the concomitant transfer of electrons from a solution-solubilized electron donor D, yields an anodic photocurrent (Figure 1 A). In contrast, transfer of the conduction-band electrons to a solution-solubilized electron acceptor, followed by the supply of electrons from the

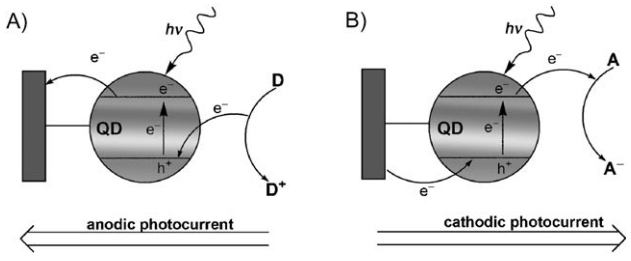

Figure 1. Photocurrents generated by semiconductor NPs associated with electrodes: A) anodic photocurrent, B) cathodic photocurrent.

[*] R. Gill, Dr. M. Zayats, Prof. I. Willner
Institute of Chemistry, The Hebrew University of Jerusalem
Jerusalem 91904 (Israel)
Fax: (+972) 2-6527-715
E-mail: willnea@vms.huji.ac.il
Homepage: http://chem.ch.huji.ac.il/willner

electrode to neutralize the valence-band holes, yields a cathodic photocurrent (Figure 1B). Numerous studies on the assembly of semiconductor QDs on surfaces and the photoelectrochemical functions of the systems have been examined. For example, monolayers and multilayers of cadmium sulfide nanoparticles were fabricated on a gold substrate covered with alkanedithiol self-assembled monolayers (SAMs) by alternate immersion of the substrate into ethanolic solutions of dithiols (1,6-hexanedithiol or 1,10-decanedithiol), and dispersion of CdS nanoparticles (ca. 3 nm in diameter), the latter of which were prepared in sodium bis(2-ethylhexyl)sulfosuccinate (Aerosol OT, AOT)/H_2O/heptane reversed micelles.[11] Photocurrent action spectra of the electrode were recorded in the presence of triethanolamine as an electron donor. In another example, very high photocurrent quantum yields were achieved when CdS nanoparticles were attached to carbon nanotube (CNT)-modified gold electrodes.[12] The photoelectrochemical functions of semiconductor QD assemblies on electrode supports were extensively studied for the development of solar cells that convert solar light energy into electrical power.[13–16]

QDs, with their unique fluorescence properties and photoelectrochemical functions, are photoactive materials for the development of sensor systems. For example, a CdSe/ZnS dual QD system was used to measure potassium ions in aqueous solutions.[17] Two quantum dots of different sizes were employed: a 3.2 nm QD ($\lambda_{em} = 545$ nm) served as the energy donor, and a 5.6 nm particle ($\lambda_{em} = 635$ nm) as the energy acceptor. A [15]crown-5 ether receptor was bound to each particle using a lipoic acid linker. The crown ether showed selectivity for potassium ions and formed a QD (545 nm):K^+:QD (635 nm) sandwich complex upon addition of the metal ion. Formation of the complex resulted in the differently sized quantum dots coming close enough together to engage in energy transfer. A ratiometric response was therefore realized upon increasing the levels of potassium ions, the emissions at 545 nm and 635 nm decrease and increase, respectively. In a different example, a ratiometric QD-based pH sensor was synthesized by attaching a pH-sensitive squaraine dye to the surface of the QDs.[18] Temperature sensing is an intrinsic property of QDs, and (CdSe)ZnS QDs in poly(lauryl methacrylate) matrices show linear and reversible changes in the fluorescence in the temperature range of 315 to 100 K.[19]

QDs show great promise as photonic labels for bioanalytical applications. The similar dimensions of QDs and biomaterials, such as enzymes, antigens/antibodies, protein receptors, or nucleic acids, suggest that electronic communication between the QDs and the specific recognition site or biocatalytic processes of the biomaterials in the hybrid nanosystems may exist. These electronic interactions may lead to the optical or photoelectrochemical transduction of the biological events. Furthermore, the incorporation of the biomaterial/QDs hybrid nanostructures into cellular environments could combine the targeting functions of the biomolecules with the superior photophysical properties of QDs to explore and control intracellular processes.

Substantial progress has been made in the utilization of semiconductor QDs as optical labels or photoelectrochemical and electrochemical transduction elements for the sensing of biorecognition and biocatalytic processes. Recent review articles summarize the progress in the application of the fluorescence properties of QDs in bioanalysis.[20–22] Herein, however, the emphasis will lie on the use of the QDs as optical labels that follow dynamic biochemical transformations, or as photoelectrochemical transduction means for biorecognition events or biocatalytic transformations.

2. Water Solubilization and Functionalization of Quantum Dots with Biomolecules

The superior photophysical features of semiconductor QDs (high fluorescence quantum yields and stability against photobleaching) are usually observed in organic solvents, and their introduction into aqueous media is usually accompanied with a drastic decrease in the luminescence yields of the QDs. This effect presumably originates from the reaction of surface states with water, a process that yields surface traps for the

Ron Gill is a Ph.D. student in the laboratory of Professor I. Willner. His research interests include the application of semiconductor nanoparticles in bioanalysis, and the development of biosensors. He is a Clore Foundation Fellow and received the Wolf Prize for Ph.D. students.

Maya Zayats completed her Ph.D. studies under the supervision of Professor I. Willner at the Hebrew University of Jerusalem in 2007. Her research interests include the development of electronic biosensors and the application of nanoparticles in bioanalysis. She received the Eshkol Fellowship (Israel Ministry of Science) and the Yashinski Award.

Itamar Willner completed his Ph.D. studies at the Hebrew University of Jerusalem in 1978. After postdoctoral research at the University of California, Berkeley, he joined the Hebrew University of Jerusalem as Professor. His research interests include bioelectronics, nanobiotechnology, synthesis and applications of metal or semiconductor nanoparticles, electrochemistry, and photochemistry. He received the Israel Prize in Chemistry (2002), the Rothschild Prize (2008), and is a member of the Israel Academy of Sciences and Humanities and the European Academy of Sciences and Arts.

conduction-band electrons.[23] As biorecognition events or biocatalytic transformations require aqueous environments as the reaction media, it is imperative to preserve the luminescence properties of the QDs in aqueous systems. Methods to stabilize the fluorescence properties of semiconductor QDs in aqueous media have been reported, including surface passivation with protective layers, such as proteins,[24,25] and the coating of the QDs with protecting silicon oxide films[26,27] or polymer films.[1,28,29] Although these methods successfully preserve the photophysical properties of the QDs, the passivation layers prevent the useful application of the QDs in bioanalysis that involve following dynamic biochemical processes.

Quantum dots can be employed as optical labels that probe dynamic biological processes, such as biocatalyzed reactions or structurally induced biomolecular transformations, using fluorescence resonance energy transfer (FRET) or electron-transfer quenching as photophysical probing mechanisms.[30,31] The sensitivity of these photophysical processes to the distance separating the donor–acceptor or chromophore–quencher pairs prevents, however, the use of the passivated fluorescent QDs as optical probes for dynamic bioprocesses because of the thick stabilizing capping layers associated with the nanoparticles. Thus, a delicate balance between the nanostructure of the modifying capping layer associated with the QDs and its effect on the photophysical features of the particles must be maintained. Several methods to synthesize water -soluble QDs that retain high fluorescence yields of the particles have been reported.[20,32,33] These methods use water-soluble molecular or macromolecular capping agents that associate with the surface of the QDs by covalent or ligand–ion interactions to yield monolayer or thin-film capped particles (Figure 2). For example, CdSe QDs with a narrow size distribution that reveal a high fluorescence quantum yield (25%) were synthesized by a single-step procedure in water using glutathione (GSH) as a stabilizing agent.[34] Similarly, glutathione-capped CdTe (GSH-CdTe) QDs with tunable fluorescence (500–650 nm) and quantum yield as high as 45% were synthesized in aqueous media and employed for the staining of fixed cells.[35] The single-step synthesis of thiolated cyclodextrin-modified CdSe/CdS core-shell QDs resulted in water-soluble QDs with a quantum yield of 46% in water.[36]

Another method for the preparation of water-soluble QDs relies on the exchange of native organic ligands linked to the QD, such as trioctylphosphine oxide (TOPO) or octadecylamine (ODA), with thiolated water-soluble ligands in a water-organic two-phase system. The most common thiolated molecules used to stabilize semiconductor QDs in aqueous media are thiolated aliphatic carboxylic acids, such as mercaptoacetic acid (MAA),[25,37,38] mercaptopropionic acid (MPA), or mercaptoundecanoic acid (MUA). To achieve higher stability, bidentate surface ligands composed of derivatives of dihydrolipoic acid (DHLA) were used for the preparation of water-soluble CdSe/ZnS QDs.[24,39] The DHLA ligands provide stable interactions with the QD surfaces owing to the bidentate chelate effect of the dithiol groups. Also, lipoic acid units tethered to poly(ethylene glycol) spacers that were functionalized with linkable functionalities for biomolecules were used to modify the QDs.[40,41] These modifiers eliminate nonspecific adsorption processes and also provide anchoring sites for the covalent immobilization of the biomolecules. Other thiol-containing materials, such as peptides with a polycysteine adhesive domain, were used to synthesize water-soluble QDs.[42,43] Recently, QDs were stabilized by exchanging ODA with water-soluble dendrons to yield water-soluble QDs with quantum yields of 36%.[44] Interestingly, internally facing carboxylate groups on the dendrons retained a higher

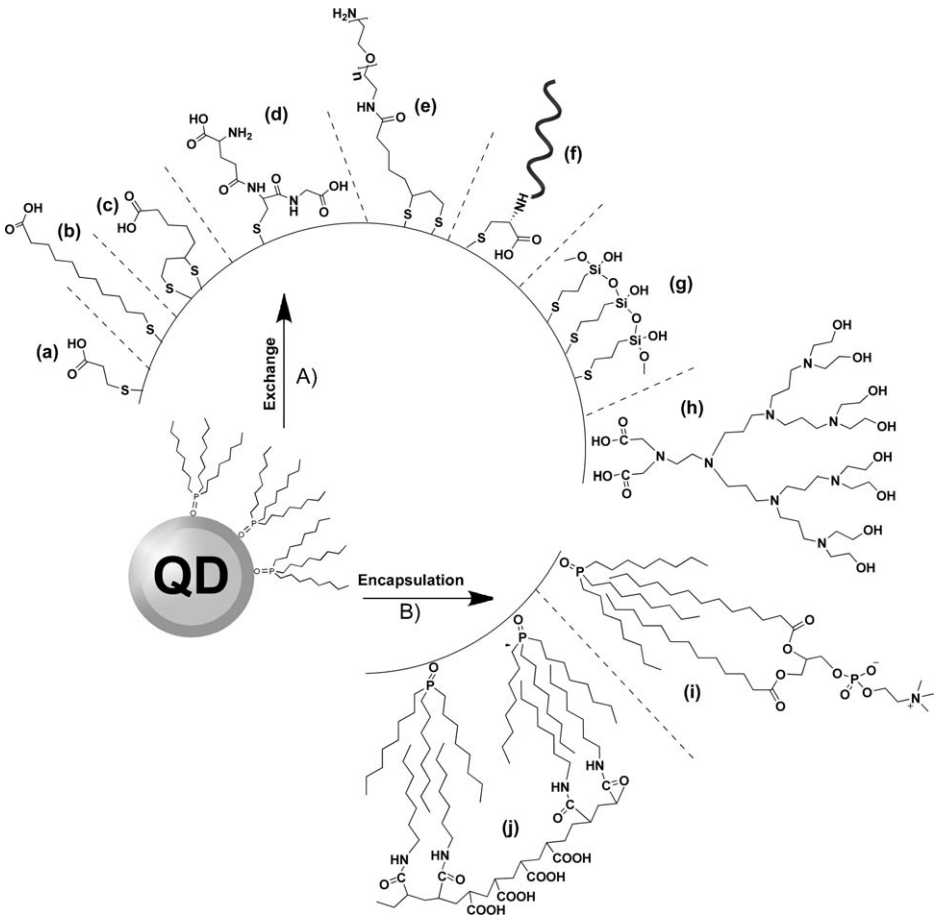

Figure 2. Modification of semiconductor QDs with functional encapsulating layers for water solubilization and preservation of luminescence properties and/or secondary covalent modification of the surface with biomolecules. A) Exchange of the organic encapsulating layer with a water-soluble layer; a)–d) thiolated or dithiolated functional monolayers, e) glutathione layer, f) cysteine-terminated peptide, g) thiolated siloxane, h) carboxylic acid-functionalized dendrone. B) Encapsulation of QDs stabilized with an organic encapsulating layer in functional bilayer films composed of i) a phospholipid encapsulating layer, and j) a diblock copolymer.

quantum yield in water compared with an internally facing thiol group.[45] Instead of exchanging the organic capping layer used in the synthesis of the particles, amphiphilic polymers can be used that have both a hydrophobic side chain that interacts with the organic capping layer and a PEG backbone for water solubility.[46,47] Such QDs retained their quantum yields (55%) upon transfer to aqueous media.

Several methods have been used for the attachment of biomolecules to quantum dots. The most common methods involve the coupling of primary amines tethered to the biomolecules to carboxylic acid residues on the encapsulating layer associated with the nanoparticles. Although this method is suitable for DNA modified with a single primary amino group at its end,[48] it may lead to crosslinking, and even aggregation, when used with proteins that contain carboxylic and amine residues. Proteins engineered to have a positively charged domain,[24] or positively-charged proteins, such as avidin[49] or papain,[50] can be electrostatically attached to the negative surface of carboxylic acid-modified QDs. Antibodies that include free exposed thiol groups, after reduction with DTT, were conjugated to QDs that have free amine functionalities in their capping layer using heterobifunctional crosslinkers, such as succinimidyl 4-(*N*-maleimidomethyl)cyclohexane-1-carboxylate (SMCC).[51] A polyhistidine tag consisting of six histidine residues binds carboxy-functionalized QDs. By adding a polyhistidine tag to proteins,[41,52] antibodies,[53] short peptides,[54] and DNA,[55] assembly of these biomolecules on surfaces of QDs was achieved.

The capping layer associated with the QDs not only preserves the photophysical properties of the nanoparticles, but often enables the modification of electrodes with QDs. For example, CdS nanoparticles modified with 2-aminoethanethiol and 2-mercaptoethanesulfonate were covalently coupled to a 3,3′-dithiobis(succinimidyl propionate)-modified gold electrode.[56] Tunneling spectroscopy (TS) of a single particle whose size was determined from a scanning tunneling microscopy (STM) image successfully allowed the determination of the band-gap energy of the size-quantized particle. Similarly, CdS nanoparticles capped with *p*-aminothiophenol were electrochemically polymerized into a gold electrode functionalized with a *p*-aminothiophenol monolayer.[57] Photocurrents generated by the electrode in the presence of triethanolamine are strongly dependent on the redox state of the dianiline bridging unit. Alternatively, CdSe QDs capped with mercaptopropionic acid were covalently bound to 11-amino-1-undecanethiol self-assembled monolayers on gold electrodes.[58] The process was followed by surface plasmon resonance (SPR), and it was found that binding saturates at submonolayer coverage. Instead of using covalent binding, hydrogen bonds have been used to assemble CdS NPs on electrodes, using barbiturate-based thiolated compounds on both the NPs and the electrodes.[59]

3. Semiconductor Quantum Dots as Optical Labels for Bioanalysis

Functionalized semiconductor QDs have been used as fluorescence labels in numerous biorecognition events,[60–65] such as immunoassays for protein detection (Figure 3A) or the analysis of nucleic acids (Figure 3B). For example, CdSe/ZnS QDs were functionalized with avidin groups and used as

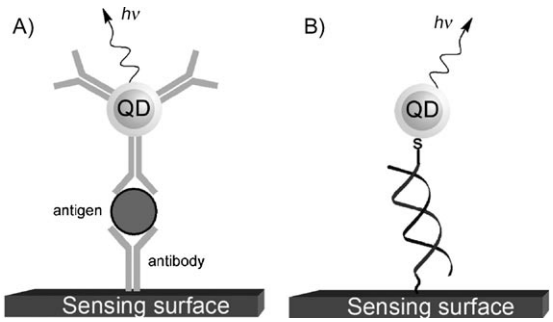

Figure 3. The fluorescent analysis of: A) an antigen by antibody-functionalized QDs, and B) DNA by a nucleic acid-functionalized QD.

fluorescent labels for biotinylated antibodies. Fluoroimmunoassays utilizing these antibody-conjugated NPs were successfully used in the detection of protein toxins (staphylococcal enterotoxin B and cholera toxin).[49,66] Similarly, CdSe/ZnS QDs conjugated to appropriate antibodies were applied for the multiplexed sandwich fluouroimmunoassay for the simultaneous detection of four toxins (cholera toxin (CT), ricin, shiga-like toxin 1 (SLT), and staphylococcal enterotoxin B (SEB)) by using differently sized QDs (Figure 4A), and performing the reaction in single wells of a microtiter plate, in the presence of a mixture of all four QD-antibody conjugates

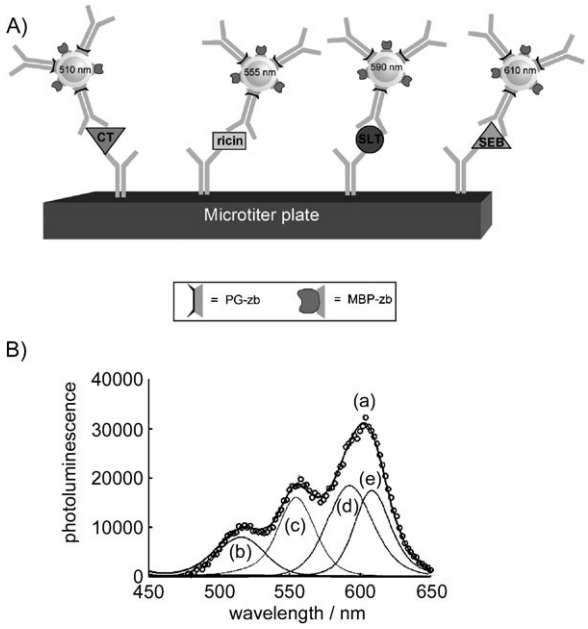

Figure 4. A) The parallel optical analysis of antigens in a well array using the fluorescence of differently sized quantum dots. B) The fluorescence spectrum observed for the four analytes (concentration: 1 μg mL^{-}) by the differently sized QDs (a), and deconvoluted spectra of individual toxins: b) CT, c) ricin, d) SLT, and e) SEB. Reprinted in part with permission from Ref. [67]. Copyright 2004 American Chemical Society.

(Figure 4B),[67] thus leading to the fluorescence that encodes for the toxins. In another example, multiplexed immunoassay formats based on antibody-functionalized QDs were used for the simultaneous detection of *Escherichia coli* O157:H7 and *Salmonella typhimurium*[68] and for the discrimination between the diphtheria toxin and the tetanus toxin proteins.[69] This was achieved by the modification of QDs having two different emission wavelengths with the respective antibodies.

Conventional DNA fluorescent microarrays are based on the sandwich hybridization of target DNA between a capture probe attached to a surface and a fluorophore-modified signaling probe. Recently, the use of DNA-functionalized QDs as signaling probes for DNA microarrays was demonstrated. Fluorescent QDs were used for the detection of single-nucleotide polymorphism in human oncogene p53 and for the multiallele detection of the hepatitis B and the hepatitis C virus in microarray configurations.[70] DNA-functionalized CdSe/ZnS QDs of different sizes were used to probe hepatitis B and C genotypes in the presence of a background of human genes. The discrimination of a perfectly matched sequence of the p53 gene in the presence of background oligonucleotides that included different single-nucleotide polymorphism sequences was detected with true-to-false signal ratios higher than 10 (under stringent buffer conditions) within minutes at room temperature.

QDs were also used for microRNA detection in a microarray configuration.[71] Streptavidin-conjugated QDs were used to label miRNA targets biotinylated at their 3′ termini, and hybridized with the corresponding complementary DNA probes immobilized on glass slides. The resulting fluorescence from the QDs that labeled the miRNAs was then used as readout signal (Figure 5A). Analysis of a model system indicated that the detection limit for analyzing miRNA was about 0.4 fmol and the detection dynamic range spanned across two orders of magnitude, from 156 to 20000 pM (Figure 5B). The method was applied to develop an assay for profiling 11 miRNA targets from rice (Figure 5C). Additionally, siRNA screening was accomplished by using QD-conjugated hybridization probes, together with mRNA amplification and Cy5 labeling. Hybridization between the Cy5-labeled mRNA sense sequence and the siRNA antisense sequence conjugated to the QD was followed by FRET analysis.[72]

DNA/QDs conjugates were used as fluorescence probes for the fluorescence in situ hybridization (FISH) assays. In such assays, genomic DNA is denaturated and then allowed to hybridize with a fluorescent-labeled DNA sequence to visualize the presence or absence of specific DNA sequences in the chromosomes. For example, the QD-based FISH labeling method was used for the detection of the Y chromosome in human sperm cells.[73] Similarly, the QDs-based FISH method to analyze human metaphase chromosomes was reported.[74] The researchers showed that QD-labeled DNA gave a higher signal-to-noise ratio and was more photostable than commonly used fluorophores, such as FITC and Texas Red (Figure 6A). To show its applicability to clinically important disease genes, the researchers used the

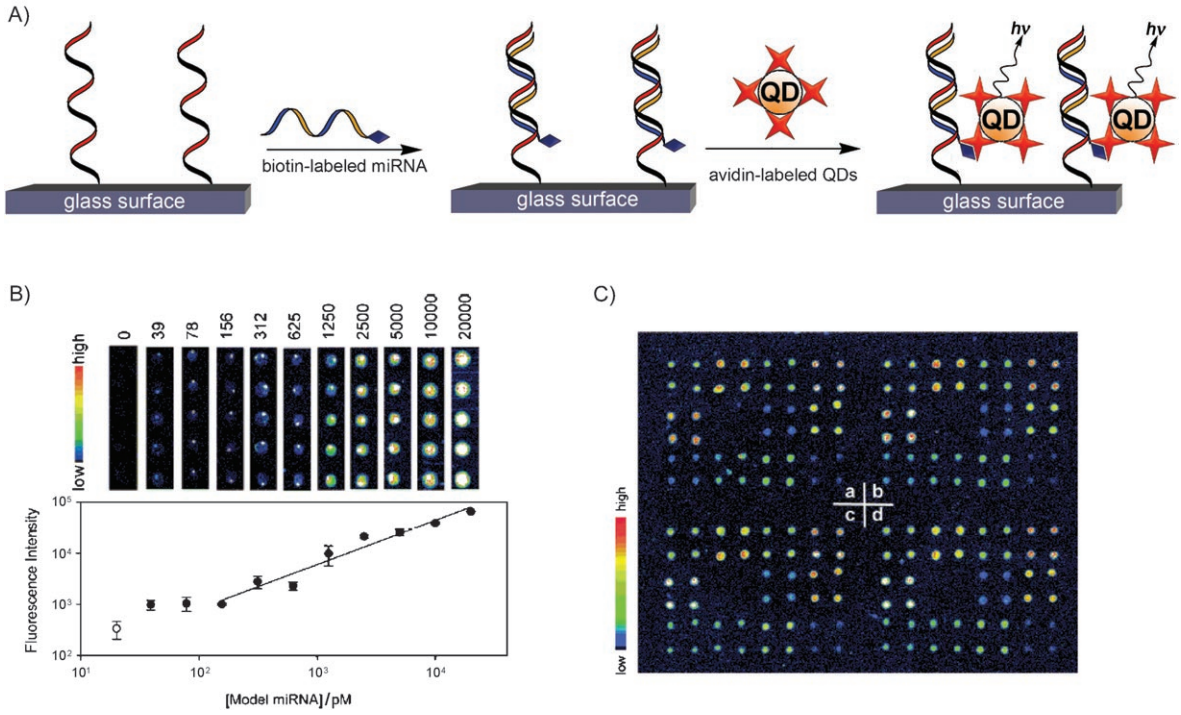

Figure 5. Analysis of miRNA by means of fluorescent QDs. A) Organization of the streptavidin-labeled QDs on a DNA/miRNA duplex bound to a glass support. B) Fluorescence intensities detected upon analyzing different concentrations of a target miRNA (upper panel), and derived calibration curve (lower panel). C) Analysis in an array format of 11 target miRNAs from rice. Reprinted in part from Ref. [71] with permission of the Oxford University Press.

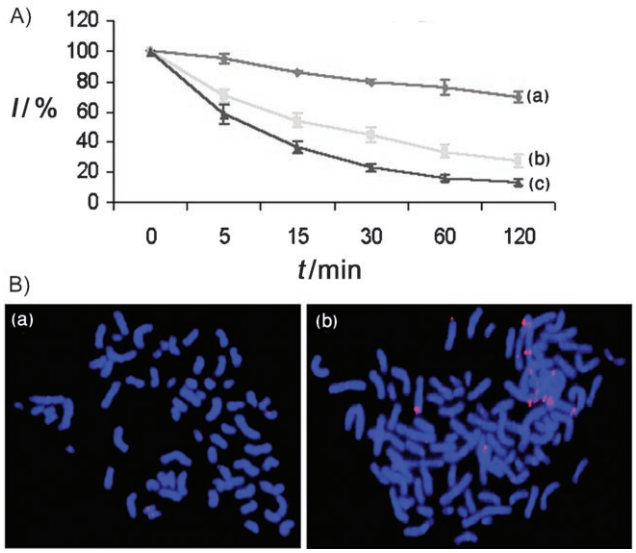

Figure 6. A) Comparison of the photostability of the QD–nucleic acid/chromosome hybrid (a) with the stability of Texas Red (TR) nucleic acid/chromosome (b), and fluorescein isothiocyanate (FITC)-fuctionalized nucleic acid/chromosome (c). B) FISH imaging of a) HER2 gene-low copy human lymphocytes, and b) HER2 gene-amplified SK-BR-3 breast cancer cells by nucleic acid functionalized QDs complementary to the HER2 gene. Reprinted in part from Ref. [74] with permission of the Oxford University Press.

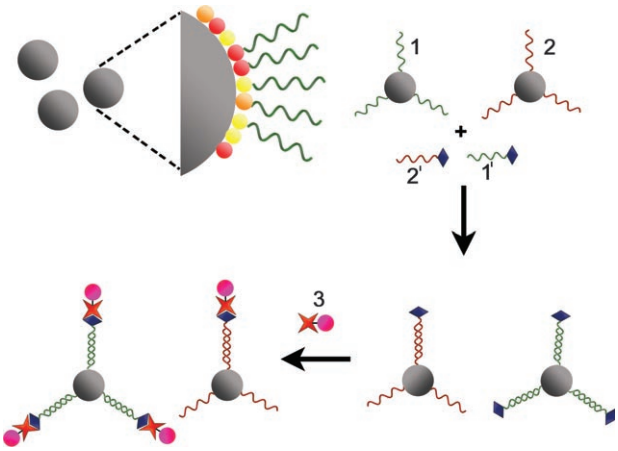

Figure 7. Multiplexed analysis of cRNAs using QD–bead composites as capturing codes and an IR-emitting QD–avidin hybrid as a versatile optical reporter unit. Adapted in part from Ref. [77]. Copyright 2006 American Chemical Society.

QD-labeled DNA for the detection of the human epidermal growth factor receptor 2 (HER2) gene (Figure 6B), which is an oncogene related to breast cancer. Approximately 25–30% of breast cancers will have a high copy number of this gene, and it is associated with increased disease recurrence. The FISH technique was also used for the multiplex cellular detection of different mRNA targets,[75] and was used to visualize a pUC18 plasmid inside *Escherichia coli* HB101 bacteria.[76]

Signal enhancement and multiplexed analysis was achieved by QDs attached to beads, or QDs incorporated in polymer bead matrices. The attachment of many QDs to a single bead results in the enhancement of the emitted light signal, and the use of differently sized QDs, and in particular, ratios of differently sized QDs, allows multiplexed analysis by the QD-encoded beads. Gene expression was analyzed by QDs that were linked to magnetic microbeads (Figure 7).[77] QDs of different sizes were attached at various ratios onto different magnetic microbeads. The spectrum of the resulting microparticle provided an optical code for the specific composition of the particles. The QD-functionalized particles each included the substitution of the QD coding with a specific capturing nucleic acid. In the specific example, two magnetic beads, each with a different QD code, are functionalized with two different nucleic acids, **1** and **2**, on their QD codes. In the presence of the biotinylated cRNA analytes, **1′** and **2′**, hybridization to the functionalized microbeads occurs. The hybridization events are then transduced using a versatile tracer composed of an IR-emitting QD linked to avidin (**3**). The readout of the hybridized cRNAs is then accomplished on a surface using the IR-emitting QDs as tracer units for the microparticles that underwent hybridization. The subsequent optical detection of the respective codes enables the identification of the nucleic acid that participated in the hybridization. The method enabled not only the multiplexed analysis of different cRNAs, but also the quantitative measurement of gene expression by monitoring the IR-QD emitted light intensity. QD composite beads were also used for the detection of DNA hybridization using a dye as a tracer unit.[78] Alternatively, sandwich assay formats used antibody-coated QD–bead composites and a dye-labeled antibody as reporter element. These latter systems were employed for the detection of different markers involved in infectious diseases[79] and autoantibodies.[80]

Different sensing schemes have been developed in which QDs were used as FRET donors. A common method for FRET-based sensing of an analyte involves the displacement of a bound quencher.[81] For example, the association of maltose to the hybrid composed of the maltose-binding protein was examined by the application of a CdSe/ZnS QD linked to the maltose binding protein (MBP).[39] These particles were interacted with a β-cyclodextrin–QSY-9 dye conjugate, resulting in the quenching of the QDs luminescence (Figure 8A). Displacement of the dye-labeled sugar from the protein upon addition of maltose resulted in the regeneration of the luminescence of the QDs (Figure 8B). This method enabled the development of a competitive QD-based sensor for maltose in solution.

A competitive QD-based assay for the detection of the explosive trinitrotoluene (TNT) has also been developed.[82] CdSe/ZnS QDs were functionalized with a single-chain antibody fragment that selectively binds TNT. The analogous substrate trinitrobenzene (TNB) was covalently linked to the quencher dye BHQ10 (**4**) and was bound to the QD/antibody conjugate; the associated substrate quenched the fluorescence of the QDs (Figure 9A). In the presence of the TNT analyte, the quencher TNB-BHQ10 conjugate was competitively displaced. This eliminated the FRET process between the QD and the dye, and switched on the fluorescence of the

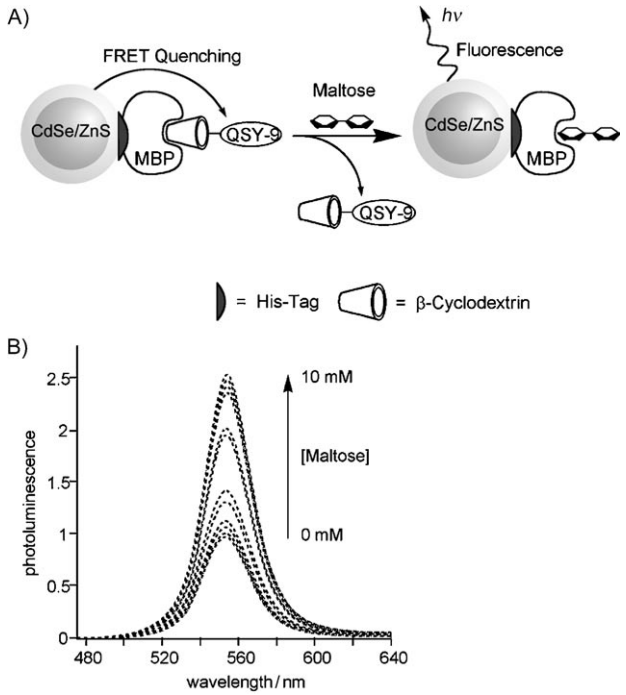

Figure 8. A) CdSe/ZnS QDs for the competitive assay of maltose using the maltose binding protein (MBP) as sensing material and β-cyclodextrin–QSY-9 dye conjugate β-CD-QSY-9 as FRET quencher. B) The fluorescence changes of the MBP-functionalized QDs with increasing concentrations of maltose. Reprinted by permission from Macmillan Publishers Ltd, Nature Materials, Ref. [39].

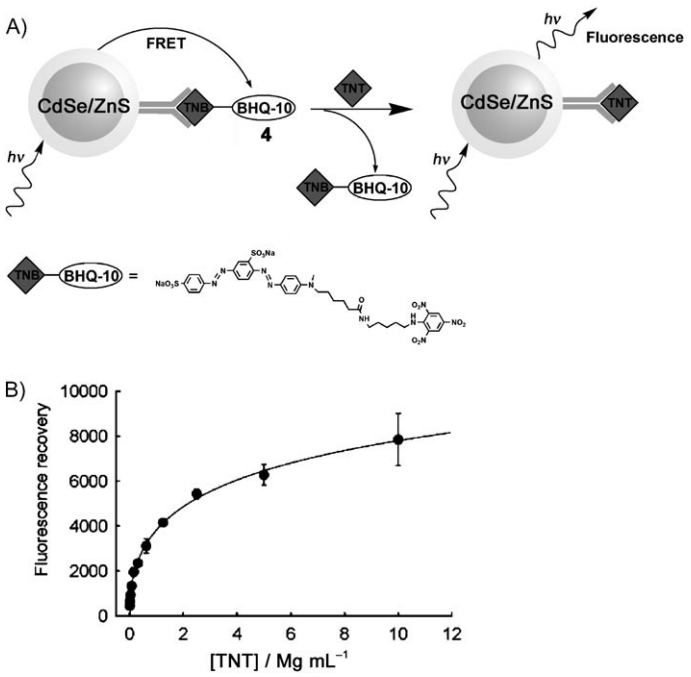

Figure 9. A) Competitive analysis of TNT by the anti-TNT antibody associated with CdSe/ZnS QDs and using BHQ-10 as quencher. B) Derived calibration curve for the analysis of TNT. Reprinted with permission from Ref. [82]. Copyright 2005 American Chemical Society.

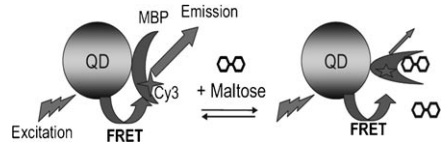

Figure 10. Control of the FRET process between CdSe and Cy3-functionalized maltose binding protein (MBP) upon association of maltose and induction of a conformational change in MBP. (From Ref. [84]).

QDs (Figure 9B). Competitive QD-based assays were also used for the detection of glycoproteins.[83]

Another method for FRET-based biosensing involves the structural changes of proteins upon interaction with their substrates. This method was used for the assembly of a reagent-free QD-based sensor for maltose.[84] CdSe/ZnS QDs were functionalized with the maltose binding protein mutant, MBP41C, which includes a cysteine at a peristeric site that does not take part in the maltose binding properties. This residue was specifically labeled with a fluorescent dye, Cy3, which acts as a FRET acceptor from the QD. Upon binding maltose, MBP undergoes conformational changes that alter the environment surrounding the dye, thus changing its fluorescence in a concentration-dependent manner (Figure 10). These conformational changes result in both the enhanced FRET from the QDs to the dye, and the enhancement of the nonradiative decay of the dye.

The hydrolytic functions of a series of proteolytic enzymes were analyzed by the application of QD-modified dye-labeled peptides that acted as reporter units for the biocatalytic transformations, and used the FRET process as a readout mechanism.[54,85–87] CdSe QDs were modified with different peptides that included peptide sequences with specific cleavage sites for different proteases, and quencher units were tethered to the termini of the peptides. The fluorescence of the QDs was quenched in the presence of the quencher-peptide capping layer. The sequence-selective hydrolytic cleavage of the peptides by the respective protease resulted in the removal of the quencher units, and this restored the fluorescence of the QDs. For example,[85] collagenase was used to cleave the rhodamine Red-X dye-labeled peptide **5** linked to CdSe/ZnS QDs (Figure 11A). Whereas the tethered dye quenched the fluorescence of the QD, the hydrolytic scission of the dye and its corresponding removal restored the fluorescence of the QDs (Figure 11B).

The hybridization of complementary nucleic acids and dynamic biocatalytic transformations on DNA were reported using QDs and FRET processes. CdSe/ZnS QDs conjugated to nucleic acids have been used to follow the biocatalyzed replication of DNA.[88] CdSe/ZnS NPs were functionalized with the DNA primer **6**, which is complementary to a specific domain of M13 mp18 DNA (**7**). Hybridization of the single-strand DNA **7** with the nucleic acid-functionalized QDs **6** was followed by the replication of the resulting duplex in the presence of polymerase and the dNTPs nucleotide mixture that included Texas Red-functionalized dUTP (**8**). This process resulted in the incorporation of the dye labels into the DNA replica (Figure 12A). The Texas Red dye was selected to act as energy acceptor, as its absorption spectrum overlaps the emission spectrum of the QDs. The FRET process from the semiconductor NPs to the incorporated dye

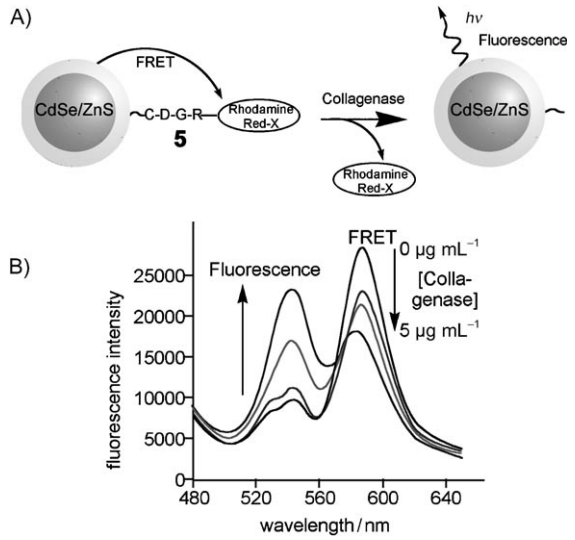

Figure 11. A) CdSe/ZnS QDs for the optical analysis of the protease-mediated hydrolysis of the rhodamine red-X-functionalized peptide **5**. B) The decrease in the fluorescence of the dye and the corresponding increase in the fluorescence of the QDs upon interaction with different concentrations of collagenase. Reprinted with permission from Ref. [85]. Copyright 2006 American Chemical Society.

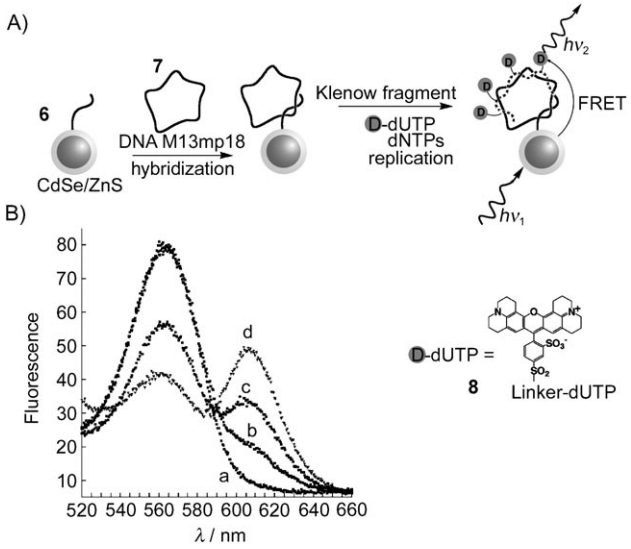

Figure 12. A) The optical detection of M13 phage DNA **7** by nucleic acid functionalized CdSe/ZnS QDs. The replication of the analyte in the presence of the dNTPs mixture with Texas-Red-labeled dUTP **8** results in the incorporation of the dye into the replica and stimulates a FRET process. B) Time-dependent fluorescence changes upon incorporation of the dye **8** into the DNA replica and the analysis of the M13 phage DNA after a) 0, b) 10, c) 30, and d) 60 min. Reprinted with permission from Ref. [88]. Copyright 2003 American Chemical Society.

units resulted in emission from the dye, with the concomitant quenching of the fluorescence of the QDs (Figure 12B). This process not only enabled the primary hybridization of the analyte DNA **7** with the nucleic acid probe **6** to be detected and amplified, but also allowed the dynamics of the time-dependent replication process to be followed.

A similar approach was used to follow telomerase activity, as telomerase is considered as an important cancer marker. The telomeres are sequences composed of G-rich constant repeat units that protect the genetic information in the chromosomes. During the cell life cycle, the telomeres are shortened, and at a certain chain length an intracellular signal that terminates cell proliferation is activated.[89,90] In certain cells the telomerase, a ribonucleoprotein, is accumulated, which results in the elongation of the telomere chains parallel to their natural shortening; as a result, immortal cells are formed. In over 95% of various cancer cells, elevated amounts of telomerase have been observed, and the enzyme is considered as a versatile marker for malignant or cancerous cells.[91,92] To analyze telomerase activity, CdSe/ZnS QDs were modified with the nucleic acid primer **9** that is recognized by telomerase (Figure 13A). In the presence of telomerase, and

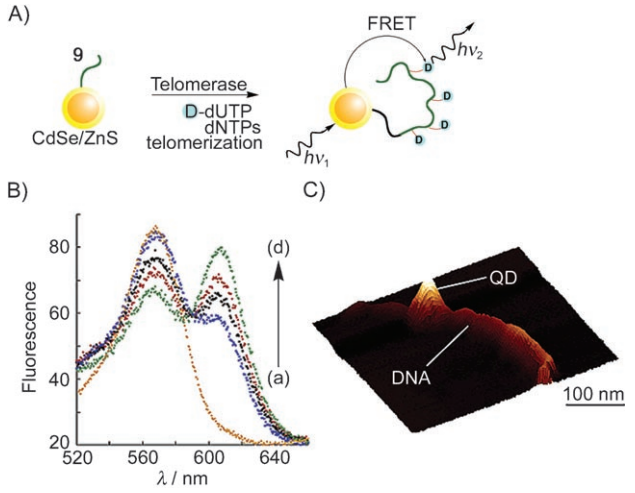

Figure 13. A) The optical analysis of telomerase activity by the incorporation of the Texas-Red–dUTP (**8**) into the telomeres associated with CdSe/ZnS QDs. B) Time-dependent fluorescence changes upon telomerization of **9**-functionalized QDs in the presence of telomerase extracted from 10000 HeLa cells, dNTPs (0.5 mM), and Texas-Red dUTP (100 μM) at time intervals of a) 0, b) 10, c) 30, and d) 60 min. (C) AFM image of the telomeres generated on the QDs. Reprinted with permission from Ref. [88]. Copyright 2003 American Chemical Society.

the nucleotide mixture dNTPs, which included Texas Red-functionalized dUTP **8**, the telomerization of the nucleic acid associated with the QDs proceeded, and the Texas-Red-labeled nucleotide was incorporated into the telomeres (Figure 13A). The FRET process from the QDs to the dye units enabled the dynamics of the telomerization process to be followed (Figure 13B).[88] Formation of telomeres on the QDs was also imaged at the molecular level using atomic force microscopy (AFM), and telomere chains as long as 300 nm were observed with the QDs, implying that about 1000 nucleotides were incorporated into the telomeric strand (Figure 13C).

The FRET quenching of CdSe/ZnS QDs was used to follow hybridization of DNA in QDs/molecular beacon (MB) conjugates.[93–95] MBs consisting of a QD and a quencher

molecule Q tethered to opposite termini of a single-strand DNA oligonucleotide hairpin structure were used. In the absence of a target DNA, the oligonucleotides existed in a hairpin structure in which the QDs and the quencher were in close proximity. In this configuration, FRET quenching of the QDs occurred, and no fluorescence from the QDs was observed. The hybridization of the target DNA with the single-strand loop of the oligonucleotide hairpin opened the stem duplex region, and the QD and quencher units adapted an extended configuration. The increased spatial separation of the QD from the quencher restored the fluorescence of the QD (Figure 14A).

For example, CdSe/ZnS QDs were linked to the 5′ end of a hairpin nucleic acid that included at its 3′ end the quencher molecule 4-(4′-dimethylaminophenylazo)benzoic acid (Dabcyl), and were used to detect single base mismatches with long-term optical stability.[93] Similarly, three differently sized CdSe/ZnS QDs were conjugated to different hairpin DNAs which were linked at their other end to the black-hole quencher-2 (BHQ2) units, and then were used in the multiplexed detection of DNAs.[94] These molecular beacons showed high target discrimination upon hybridization with the complementary target DNA, single-base-mismatched target DNA (SMT), and nonspecific DNA (NST) (Figure 14B). A 90% fluorescence intensity increase was observed in the presence of complementary target DNA relative to the system that included a nonspecific target DNA.

The FRET process occurring within a duplex DNA structure consisting of tethered CdSe/ZnS QDs and a dye was applied to probe DNA hybridization and the DNase I cleavage of the DNA.[96] CdSe/ZnS QDs functionalized with the nucleic acid **10** were hybridized with the complementary nucleic acid **11** functionalized with Texas Red (Figure 15A). The time-dependent resonance energy transfer from the QDs to the dye units was used to monitor the hybridization process. After cleavage of the double-strand DNA with DNase I, the intensity of the FRET band of the dye decreased, and the fluorescence of CdSe/ZnS QDs increased (Figure 15B). The luminescence properties of QDs only partially recovered, owing to the nonspecific adsorption of the dye onto QDs.

Aptamers are nucleic acid sequences that specifically bind proteins or low-molecular-weight substrates. The aptamers are selected from a combinatorial library of 10^{15}–10^{16} DNAs using systematic evolution of ligands by exponential enrichment (SELEX). The recognition properties of aptamers were used extensively to develop electrochemical[97,98] and optical[99,100] sensor systems. QDs were also used to probe the formation of aptamer–protein complexes.[101] An anti-thrombin aptamer was coupled to QDs, and the nucleic acid sequence was hybridized with a complementary oligonucleotide–quencher conjugate (Figure 16). The fluorescence of the QDs was quenched within the QD-aptamer/quencher-oligonucleotide duplex structure. In the presence of thrombin, the duplex was separated, and the aptamer underwent a

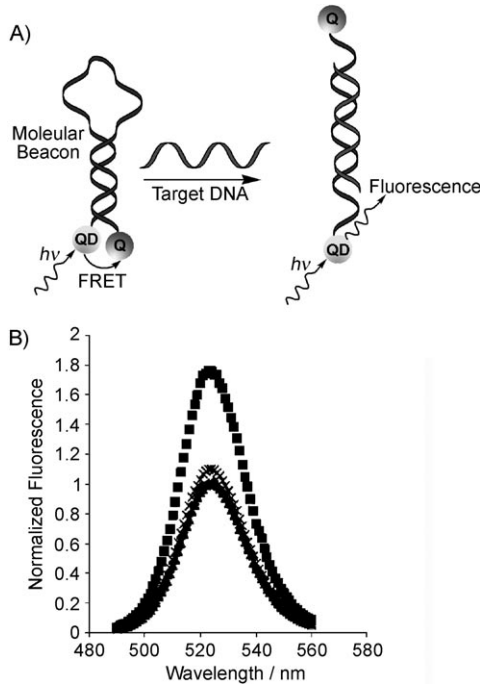

Figure 14. A) Optical detection of DNA by a hairpin nucleic acid functionalized with QDs and quencher units Q. B) Fluorescence intensities: ◆ without target DNA, ■ with target DNA: 5′-AAACCCAAACCCAAA-3′, ▲ single-base mismatched target DNA (SMT): 5′-AAACCCGAACCCAAA-3′, × non-complementary target DNA (NST): 5′-AGGTATGCTCACCTT-3′. Reprinted in part with permission from IOP Publisher Ltd. from Ref. [94]

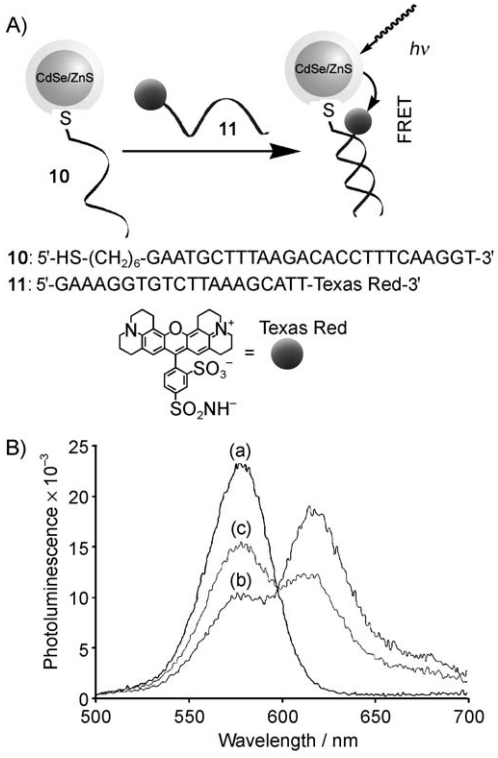

Figure 15. A) Assembly of CdSe/ZnS and Texas-Red-tethered duplex DNA. B) The fluorescence spectra of a) the **10**-functionalized CdSe/ZnS QDs, and b) the DNA duplex **10**/**11** tethered to the QDs and the Texas-Red chromophore. c) After treatment with DNase I. Reprinted with permission from Ref. [96]. Copyright 2005 American Chemical Society.

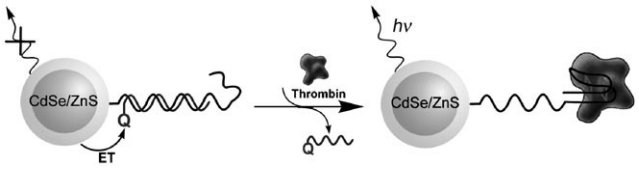

Figure 16. The analysis of thrombin by protein-induced separation of the anti-thrombin aptamer blocked by a quencher-functionalized nucleic acid that restores the fluorescence of the QDs. (Adapted in part from Ref. [101]).

conformational change to the quadruplex structure that binds thrombin. Displacement of the quencher units from the blocked aptamer activated the luminescence functions of the QDs and an approximate 19-fold increase in their fluorescence intensity was observed. In a related study, thrombin was detected by the anti-thrombin aptamer conjugated to PbS QDs.[102] Upon binding of thrombin to aptamer-functionalized QDs, selective fluorescence quenching was observed as a result of a charge-transfer process from thrombin to QDs. This method enabled thrombin to be detected at concentrations down to 1×10^{-9} M, and it showed high selectivity in the presence of high background concentrations of interfering proteins.

In addition to proteins, QD-based aptamer sensors can be used for the detection of low-molecular-weight molecules.[103] An aptamer to adenosine monophosphate (AMP; **12**) was hybridized near the 3′ end with a short nucleic acid sequence **13** which was linked to a QD, and hybridized on the 5′ end to a short nucleic acid sequence **14** attached to a gold nanoparticle, thus creating aggregates in which the fluorescence of the QD was quenched by the gold NPs (Figure 17 A). In the presence of adenosine, the aptamer underwent a conformational change, releasing the freely diffusing QDs and gold NPs. As the distance between the QDs and the gold NPs increased, the QDs regenerated their fluorescence. As the separation of the aggregate was controlled by the concentration of adenosine, the resulting fluorescence provides a quantitative signal for the analyte (Figure 17 B). A similar system was applied for the analysis of cocaine.[103]

Owing to their bright and stable fluorescence, quantum dots can be imaged at the single-particle level,[104,105] which has led to the development of an extensive research area related to biosensing at the single nanoparticle level.[105–110] One approach for single-particle detection involves the co-localization method (Figure 18). In this approach, two differently colored QDs modified with recognition sites for the analyte are passed, at high dilution, through the detector. Whereas in the absence of the analyte only the fluorescence of individual QDs is occasionally briefly observed, in the presence of the analyte, aggregation of the QDs occurs, and upon passage of the aggregate, the fluorescence of the two QDs are simultaneously activated. This method was, for example, applied for the detection of the small protein tumor necrosis factor α (TNF-α) by its antibodies.[108] Two CdSe QDs of different sizes were modified with the anti-TNF-α antibody. Co-localization of the QDs occurred in the presence of the TNF-α analyte, and upon passage of a low volume through a

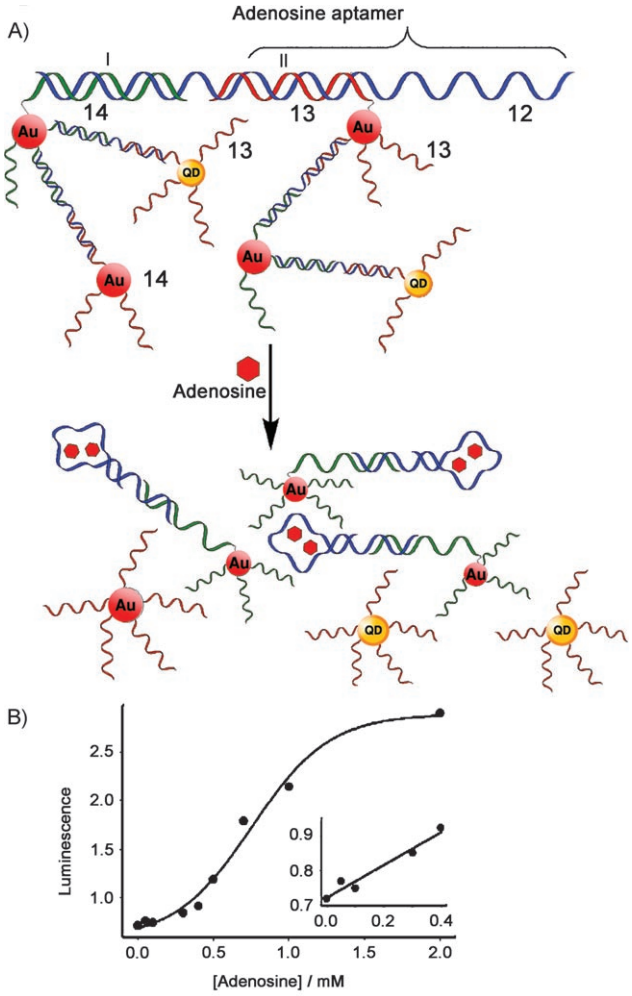

Figure 17. A) Analysis of adenosine monophosphate (AMP) by fluorescence quenching of functionalized QDs by gold nanoparticles. The anti-adenosine monophosphate aptamer **12** bridges the CdSe QD functionalized with nucleic acid **13** and the nucleic acid **14**-modified with gold NPs to form the respective aggregate. Upon analysis of AMP, the aggregate is separated, and the fluorescence of the QDs is switched on. B) Fluorescence intensity changes with respect to the concentration of AMP. Inset: enlargement of the calibration curve in the region 0.0–0.4 mM of AMP. Reprinted in part with permission from Ref. [103]. Copyright 2007 American Chemical Society.

confocal microscope detector, the fluorescence of the two QDs was initiated. A related co-localization method involved the spreading of the analyte co-localized QDs on surfaces and the imaging of the two fluorescence signals from the co-localized QDs. QD-based co-localization was also used for the detection of DNA[106–108] and whole bacteria.[108]

Another single-particle fluorescence-based method for biosensing combines FRET and the co-localization of fluorophores as the means of detection. In the presence of an analyte, a dye-labeled recognition complex is assembled on fluorescent QDs, which are then subjected, under flow, to two detector channels to simultaneously analyze the fluorescence of the QD and the FRET emission of the dye. The two emissions are observed simultaneously only if co-localization has occurred. This type of single-particle FRET (sp-FRET) sensors was applied to DNA,[109,111] and RNA/protein inter-

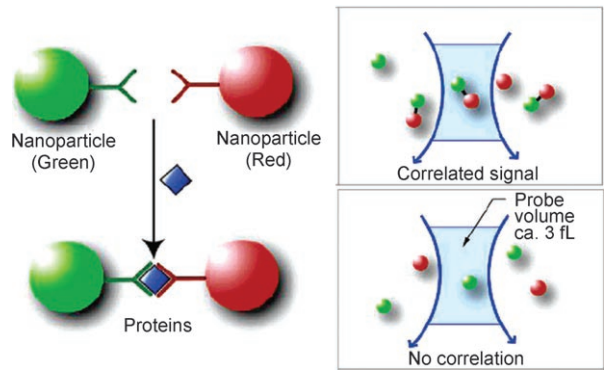

Figure 18. Analysis of TNF-α by the co-localization of two antibody-functionalized QDs of different sizes. Reprinted in part with permission from Ref. [108]. Copyright 2006 American Chemical Society.

actions.[112] For example, a target DNA **17** was sandwiched between a dye-modified reporter probe **15** and a biotinylated capture probe **16**, and assembled on streptavidin-conjugated QDs (Figure 19A).[109] Fluorescent bursts are only detected by both the donor and acceptor detection channels when the target is present (Figure 19B). This QD-based assembly had a detection limit of about 5 fM, which is almost two orders of magnitude below the sensitivity of molecular beacons under the same conditions. Interestingly, whereas the distance separating the donor–acceptor pair dominates FRET processes, it was found that FRET occurred in DNA duplexes even at relatively long distances under flow conditions. It was suggested that the double-strand DNA bends result in shorter distances between the termini-tethered donor–acceptor units, a process that enables effective FRET.[111]

Whereas the initial FRET-based biosensing schemes applied the QDs as energy donors, several recent studies have used the QDs as energy acceptors. Conventional organic dye molecules that emit at a shorter wavelength than the adjacent quantum dot do not give rise to any significant FRET process owing to the long exciton lifetime of the QD acceptor compared to that of the dye, combined with substantial direct excitation of the QD at the dye excitation wavelength.[113] This difficulty may be resolved, however, by using lanthanide complexes that exhibit long-lived luminescence lifetimes. Indeed, in a model biotin–avidin biosensing system, in which compounds were labeled with terbium (**18**) or europium complexes as donors and QDs as the acceptors, FRET was found to occur (Figure 20).[114,115] The suitablility of

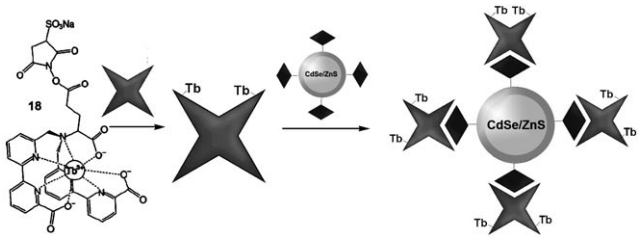

Figure 20. FRET in a hybrid assembly consisting of terbium-labeled avidin and biotinylated CdSe/ZnS QDs. Reprinted in part with permission from Ref. [115]. Copyright 2006 American Chemical Society.

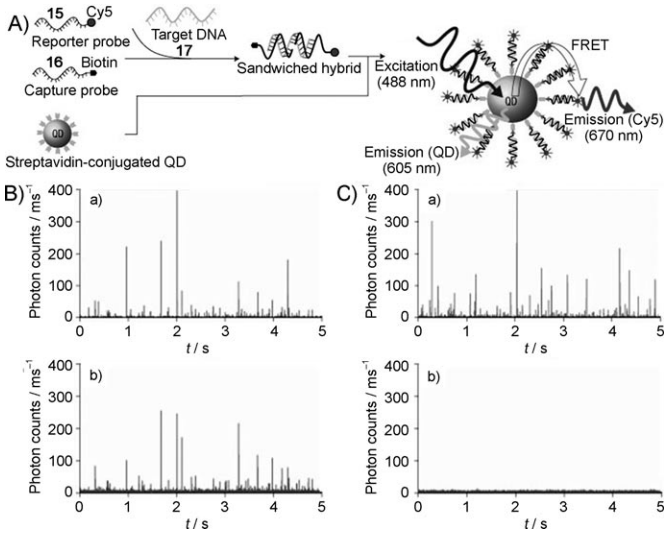

Figure 19. A) The analysis of a target DNA **17** at the single-particle level by the co-localization of a hybrid consisting of the target DNA hybridized with the probe (**15**) modified with Cy5, and the capture of nucleic acid **16**-functionalized QDs. B) Fluorescence response of the CdSe/Cy5 hybrid system in the presence of the analyte **17** (4.8×10^{-10} M) upon excitation of the QDs at $\lambda=488$ nm: a) fluorescence of the QDs at $\lambda_{em}=610$ nm, b) fluorescence of Cy5 at $\lambda_{em}=690$ nm. C) Fluorescence response of the CdSe/Cy5 hybrid system in the absence of the analyte **17** upon excitation of the QDs at $\lambda=488$ nm: a) fluorescence of the QDs at $\lambda_{em}=610$ nm, b) fluorescence of Cy5 at $\lambda_{em}=690$ nm. Reprinted by permission from Macmillan Publishers Ltd, Nature Materials, Ref. [109], copyright 2005.

lanthanide–QD pairs for sensing of biomolecules still needs to be demonstrated, as the high background fluorescence from direct excitation of the QDs is anticipated to be a fundamental limitation in these systems.

Using bioluminescence as the source of the resonance energy transfer (BRET) to the QDs solves the problems associated with an external illumination source, thus creating self-illuminating quantum dots.[116] This effect was demonstrated with Luc8, a variant of *R. reniformis* luciferase, coupled to carboxylic acid capped CdSe/ZnS quantum dots. Upon addition of coelenterazine (**19**), which is a luminescent substrate of the luciferase enzyme, emission peaks at both 480 nm (coelenterazine emission) and 655 nm (QD emission) appeared (Figure 21). This method was also applied to the sensitive detection of proteases.[117] Using genetic engineering, the short peptide **20** having 15 amino acids, including the sequence-specific substrate to the MMP-2 protease and a six-histidine tag, was fused to the C terminus of the Luc8 protein. The coordination of nickel(II) ions to the histidine tag resulted in the association of the engineered protein to the QDs, and BRET was observed upon the addition of coelenterazine to the system. Treatment of the engineered protein with MMP-2 resulted in the proteolytic scission of the peptide, which prevented the association of the Luc8 enzyme with the QDs and eliminated the BRET signal (Figure 22).

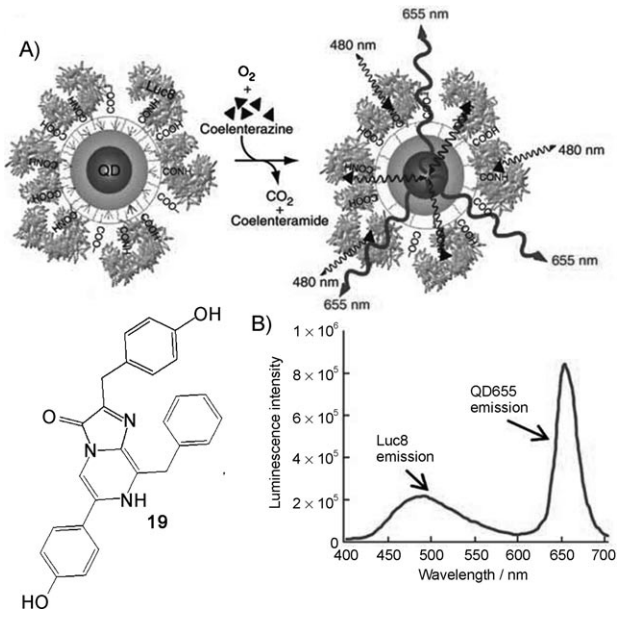

Figure 21. A) Energy transfer within a Luc8-fucntionalized CdSe QD system upon the addition of coelenterazine (**19**) and O_2. Luc8 stimulates the generation of chemiluminescence at $\lambda = 480$ nm, and the emitted light excites the QDs and results in the emission at 655 nm. B) Emission spectrum from the Luc8-fucntionalized QDs upon reaction with coelenterazine, (**19**)/O_2. Reprinted by permission from Macmillan Publishers Ltd, Nature Biotechnology, Ref. [116], copyright 2006.

Although all of the previous systems included the FRET process as the photophysical mechanism to probe biorecognition events and biocatalytic transformations, electron transfer quenching may be used as an alternative route to follow these processes. The activity of different enzymes was probed by electron-transfer quenching of semiconductor QDs.

In analogy to the analysis of the conformational changes of the maltose binding protein (MBP) upon association of maltose by the FRET process (see Figure 10), the electron-transfer quenching of CdSe QDs was used to follow the binding of maltose to MBP.[118] MBP-coated CdSe QDs were functionalized with a ruthenium complex attached to the protein, and electron-transfer quenching of the metal complex upon addition of maltose was used to sense the monosaccharide (Figure 23). Similarly, solvation changes

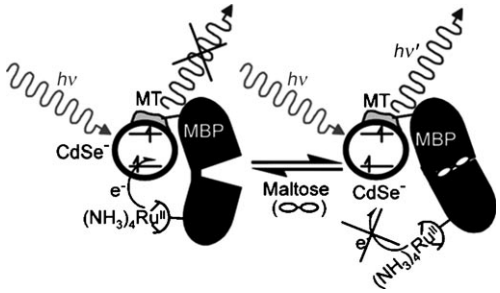

Figure 23. Controlling the degree of photoinduced electron-transfer between CdSe and MBP functionalized with $[Ru^{II}(phen)(NH_3)_4]$ upon association of maltose, and the structural alteration of the electron transfer distances. phen = phenanthroline. Reprinted with permission from Ref. [118]. Copyright 2005 American Chemical Society.

upon association of the substrate to the protein binding site could be probed by electron-transfer quenching of a ruthenium(II) complex linked close to the binding site on QDs functionalized with the binding protein. CdSe QDs were functionalized with the intestinal fatty acid binding protein that was further modified with the ruthenium(II) complex. The fluorescence changes as a result of solvation differences upon binding of fatty acids to the protein were then used to probe the analytes.[119]

In a further example, the activity of tyrosinase was analyzed by CdSe/ZnS QDs.[120] The QDs were capped with a monolayer of methyl ester tyrosine **21**. The tyrosinase-induced oxidation of the tyrosine units to the respective dopaquinone units generated active quencher units that suppressed the fluorescence of the QDs (Figure 24 A). Depletion of QD fluorescence upon interaction with different concentrations of tyrosinase was used to follow the tyrosinase activity by the time-dependent oxidation dynamics of the L-DOPA residues (Figure 24 B). Apart from demonstrating that QDs follow biocatalytic processes, the analysis of tyrosinase activity by the QDs has practical applications. Elevated amounts of tyrosinase were found in melanoma cancer cells, and thus the rapid optical detection of this biocatalytic biomarker by the QDs might be a useful diagnostic system.

The tyrosinase-stimulated oxidation of phenol residues was also employed to monitor the activity of thrombin with QDs.[120] The CdSe/ZnS QDs were func-

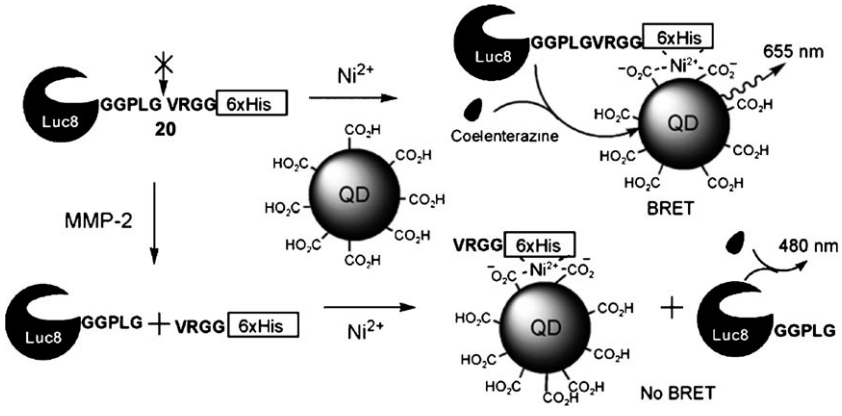

Figure 22. A) The detection of the activity of a matrix metalloproteinase (MMP) by the cleavage of the His-labeled peptide **20** tethered to Luc8 using bioluminescence resonance energy transfer to the CdSe QDs. In the absence of MMP-2, the peptide stays intact, and the bioluminescence induced by Luc8 in the presence of **19**/O_2 is detected together with the bioluminescence-induced emission of light from the QDs. In the presence of MMP-2, peptide **20** is cleaved, resulting in bioluminescence by Luc8 and **19**/O_2 only. (From Ref. [117]).

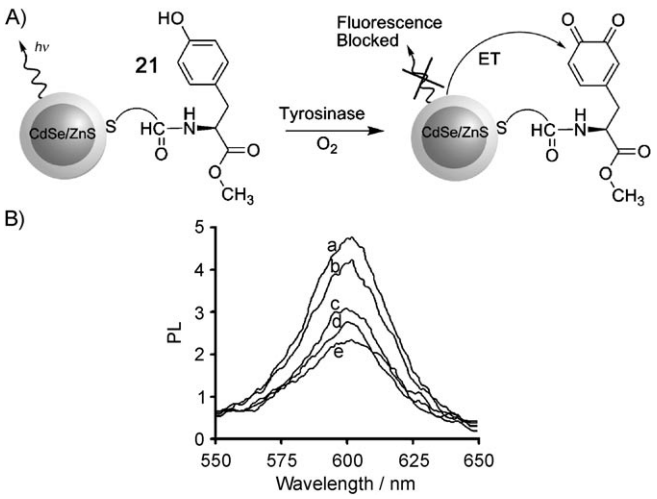

Figure 24. A) Analysis of tyrosinase activity by the biocatalytic oxidation of the methyl ester tyrosine-functionalized CdSe/ZnS QDs to the dopaquinone derivative that results in the electron transfer quenching of the QDs. B) Time-dependent fluorescence quenching of the QDs upon the tyrosinase-induced oxidation of the tyrosine-functionalized QDs: a) 0, b) 0.5, c) 2, d) 5 and e) 10 min. Reprinted in part with permission from Ref. [120]. Copyright 2006 American Chemical Society.

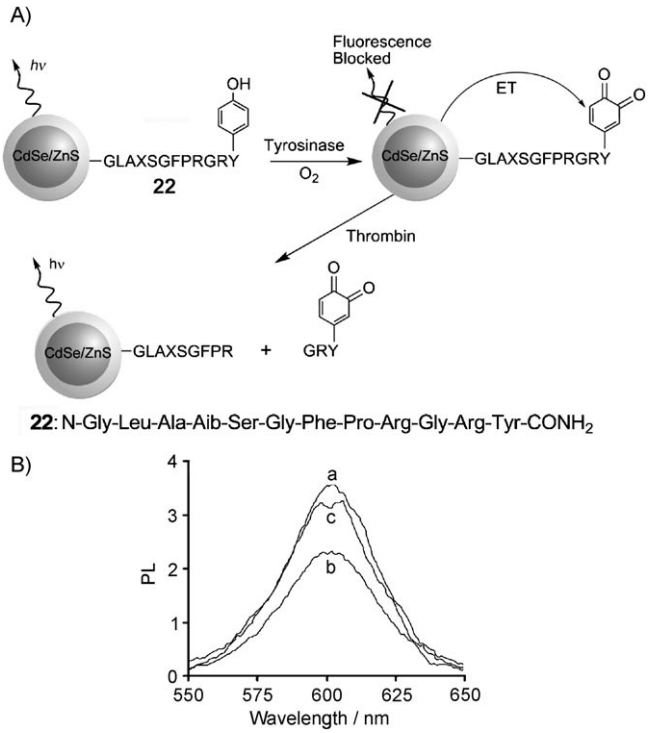

Figure 25. A) Sequential analysis of tyrosinase activity and thrombin activity by the tyrosinase-induced oxidation of the tyrosine-containing peptide **22** associated with the CdSe/ZnS QDs that results in electron-transfer quenching of the QDs, followed by the thrombin-induced cleavage of the dopaquinone-modified peptide to restore the QDs fluorescence. B) Fluorescence of QDs modified with **22** (a), after reaction of the QDs with tyrosinase for 10 min (b), and thereafter treatment of the dopaquinone-functionalized QDs with thrombin for 6 min (c). Reprinted in part with permission from Ref. [120]. Copyright 2006 American Chemical Society.

tionalized with peptide **22** that includes specific sequences for cleavage by thrombin and the tyrosine site. The tyrosinase-induced oxidation of tyrosine units yielded dopaquinone units that quenched the fluorescence of the QDs (Figure 25 A). The hydrolytic cleavage of the peptide by thrombin removed the quinone quencher units and restored the fluorescence of the QDs (Figure 25 B).

A further bioanalytical application involves the chemical control of the luminescence features of QDs by biocatalytic processes.[121] Hydrogen peroxide quenches the luminescence of CdSe/ZnS QDs, presumably by the formation of surface oxide traps of the conduction band electrons. This approach enables the quantitative analysis of H_2O_2 by QDs. These H_2O_2-sensitive QDs were then applied to develop optical biosensors for different H_2O_2-generating oxidases. For example, fluorescein-labeled avidin-functionalized CdSe/ZnS QDs were used for the optical analysis of glucose (Figure 26 A). Biotinylated glucose oxidase was linked to the particles, and the H_2O_2 product, formed upon the biocatalyzed oxidation of glucose by O_2 acted as the surface modifier of the QDs, resulting in the quenching of the luminescence. The fluorescein dye tethered to the avidin is a H_2O_2-insensitive fluorophore and acts as reference to probe the fluorescence changes of the QDs by H_2O_2. The luminescence quenching of the QDs was enhanced as the concentration of glucose was elevated, and the system enabled the quantitative ratiometric analysis of glucose (Figure 26 B). A similar approach was applied to follow the H_2O_2 generated by the acetylcholine esterase/choline oxidase cascade, and it also enabled the assay of acetylcholine esterase inhibitors by the luminescence function of the system.

4. Chemiluminescence of Semiconductor Quantum Dots for Bioanalysis

Chemiluminescence[122–124] and biochemiluminescence[125–127] are common transduction signals in bioassays. In addition to photoluminescence, cathodoluminescence,[128] chemiluminescence (CL),[129] and electrochemiluminescence (ECL)[129,130] have been observed with semiconductor quantum dots. The fact that electrochemiluminescence of QDs involves electron transfer between electrochemically generated nanocrystal species and coreactants suggests that QDs could act as ECL sensors. The major advantage of ECL analysis is the absence of any background signal that may arise from the photoexcitation of nonspecific adsorbates. Hydrogen peroxide is a biologically important coreactant to which ECL of QDs is sensitive. For example, a CdSe nanoparticle film on a paraffin-impregnated graphite electrode generated ECL upon the application of a potential (−1.2 V vs. Ag/AgCl) in the presence of H_2O_2.[131] The resulting chemiluminescence was related to the concentration of H_2O_2 in the solution (Figure 27). The detection limit was below 1 μM, with high reproducibility (relative standard deviation of 1.18 % at 10 μM H_2O_2).

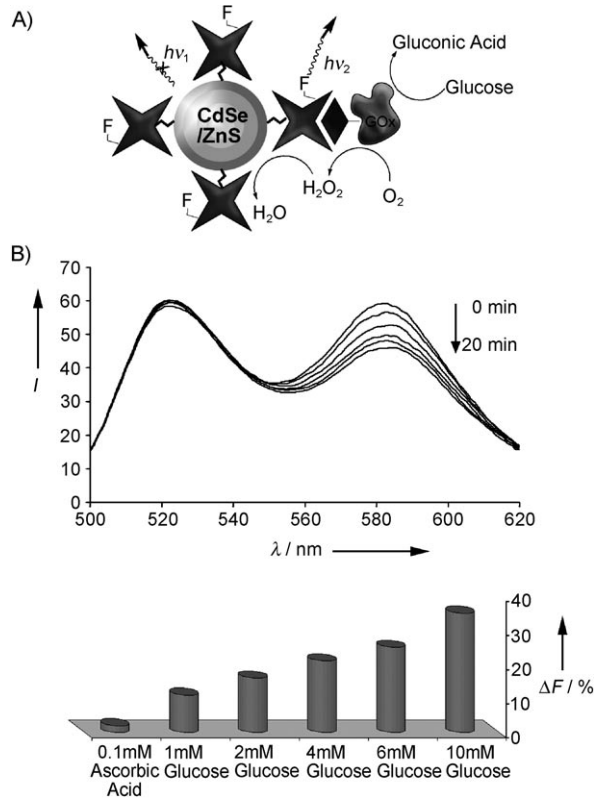

Figure 26. A) Ratiometric analysis of glucose by biotinylated GOx associated with the fluorophore-labeled avidin–CdSe/ZnS QD conjugates. B) Top: Time-dependent ratiometric fluorescence analysis of glucose (5 mM) by GOx-modified QDs after 0, 2, 5, 10, 15, and 20 min. Bottom: Quenched fluorescence of the GOx-functionalized CdSe/ZnS QDs upon analyzing different concentrations of glucose for a fixed time interval of 10 min. (From Ref. [121]).

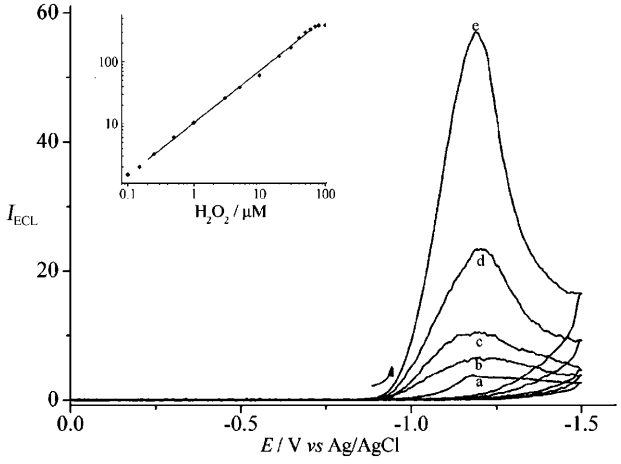

Figure 27. Potential-induced electrochemiluminescence by CdSe QDs upon addition of various concentrations of H_2O_2: a) 0, b) 0.5, c) 1, d) 3, and e) 10 μM. Inset: calibration curve. Reprinted with permission from Ref. [131]. Copyright 2004 American Chemical Society.

The proposed mechanism for the electrochemical generation of chemiluminescence in the presence of QDs and H_2O_2 is outlined in Equations (1) to (5). The electrochemical reduction of QDs yields the radical-anion charged species that react with H_2O_2 to form the hydroxyl radical as the oxidizing agent. The concomitant oxidation of the QDs by hydroxyl radicals was suggested to yield the radical cation QD species. Subsequent recombination of the radical anion and the radical cation yields excited QDs that emit light as a result of the sequence of dark reactions.

$$\text{CdSe QDs} + e^- \rightarrow R^{\bullet -} \quad R = [\text{CdSe QD}] \tag{1}$$

$$R^{\bullet -} + H_2O_2 \rightarrow R + OH^{\bullet} + OH^- \tag{2}$$

$$R + OH^{\bullet} \rightarrow OH^- + R^{\bullet +} \tag{3}$$

$$R^{\bullet -} + R^{\bullet +} \rightarrow R + R^* \tag{4}$$

$$R^* \rightarrow \text{CdSe QD} + h\nu \tag{5}$$

It is important to separate two types of ECL in quantum dots. Band-gap chemiluminescence[129,131] has a luminescence spectrum that matches the photoluminescence spectrum, and therefore is size-dependent and tuneable. Frequently, however, the chemiluminescence originates from surface states. Under these conditions, the ECL spectrum will be red-shifted and not size-dependent. Although this effect may limit applications for multiplexing, for general sensing schemes, such as H_2O_2 sensing, ECL from surface states is as efficient and sensitive as band-gap ECL.[132] Based on the electroluminescence mechanism above, ECL sensors for biologically important scavengers of hydroxyl radicals, such as GSH, were developed.[133] By quenching the hydroxyl radicals, less hole-injected QDs are created according to Equation (3), and therefore less excited QDs are produced. In addition to hydrogen peroxide, dissolved oxygen can also be an ECL coreactant by the following pathway [Eq. (6)]:

$$O_2 + 2R^{\bullet -} + 2H^+ \rightarrow 2R^* + 2H_2O_2 \tag{6}$$

Dissolved oxygen is a more efficient coreactant for ECL production than H_2O_2 at the same concentration,[134] which may explain why, in the presence of glucose oxidase and its substrate glucose, the ECL was quenched and not enhanced.

All of the ECL systems discussed above were based on cathodic ECL that occurs at very negative potentials. However, anodic ECL was shown to be useful for the detection of catechols, such as dopamine and adrenaline.[135] The oxidized catechols produced on the electrode probably quenched energy transfer rather than electron transfer, as the addition of β-mercaptoethanol to the solution, a known quencher of dopamine oxidation, caused the ECL signal to recover almost completely. Detection limits for dopamine were less than 1 μM.

Finally, chemiluminescence of a CdS NPs solution in the presence of H_2O_2 as a coreactant was shown to be sensitive to a wide variety of biological molecules and metal ions.[136]

5. Semiconductor Nanoparticles for Photoelectrochemical Bioanalysis

Photoexcitation of semiconductor QDs not only leads to luminescence properties, but the photogenerated electron–

hole species may also electrically communicate with electrode surfaces. The photoexcited QDs confined to electrode surfaces might directly communicate with the electrode surface by injection of the conduction-band electrons into the electrode, or by the sequential ejection of the conduction-band electrons to an electron acceptor solubilized in the electrolyte solution and the transfer of electrons to the valence-band holes (Figure 1). These two routes lead to the generation of an anodic photocurrent or cathodic photocurrent, respectively. Various QD–DNA hybrid systems[137–139] or QD–protein conjugates[140,141] were assembled on electrodes, and the control of the photoelectrochemical properties of the QDs by the biomolecules has been demonstrated.

A layer-by-layer deposition of nucleic acid-functionalized CdS QDs on electrodes was followed by the photoelectrochemical transduction of the assembly process.[137] The system demonstrated the amplified analysis of a DNA by photocurrent transduction. Semiconductor CdS NPs with diameters of (2.6 ± 0.4) nm were functionalized with one of the thiolated nucleic acids **23** or **24**, which are complementary to the 5′ and 3′ ends of target DNA molecule **25** (Figure 28). An array of CdS NP layers was then constructed on a gold electrode by a layer-by-layer hybridization process using the target DNA as crosslinker of CdS QDs functionalized with nucleic acids (Figure 28 A). Illumination of the array in the presence of the sacrificial electron donor triethanolamine (TEOA) resulted in the generation of a photocurrent, which increased with the number of layers of CdS NPs generated on the electrode (Figure 28 B). The photocurrent action spectra followed the absorbance features of the CdS NPs, implying that the photocurrents originated from the photoexcitation of the CdS nanoparticles. The ejection of the conduction-band electrons into the electrode occurred from the QDs that were in intimate contact with the electrode support. This hypothesis was supported by the fact that $[Ru(NH_3)_6]^{3+}$ units ($E^0 = -0.16$ V vs. SCE), which were electrostatically bound to

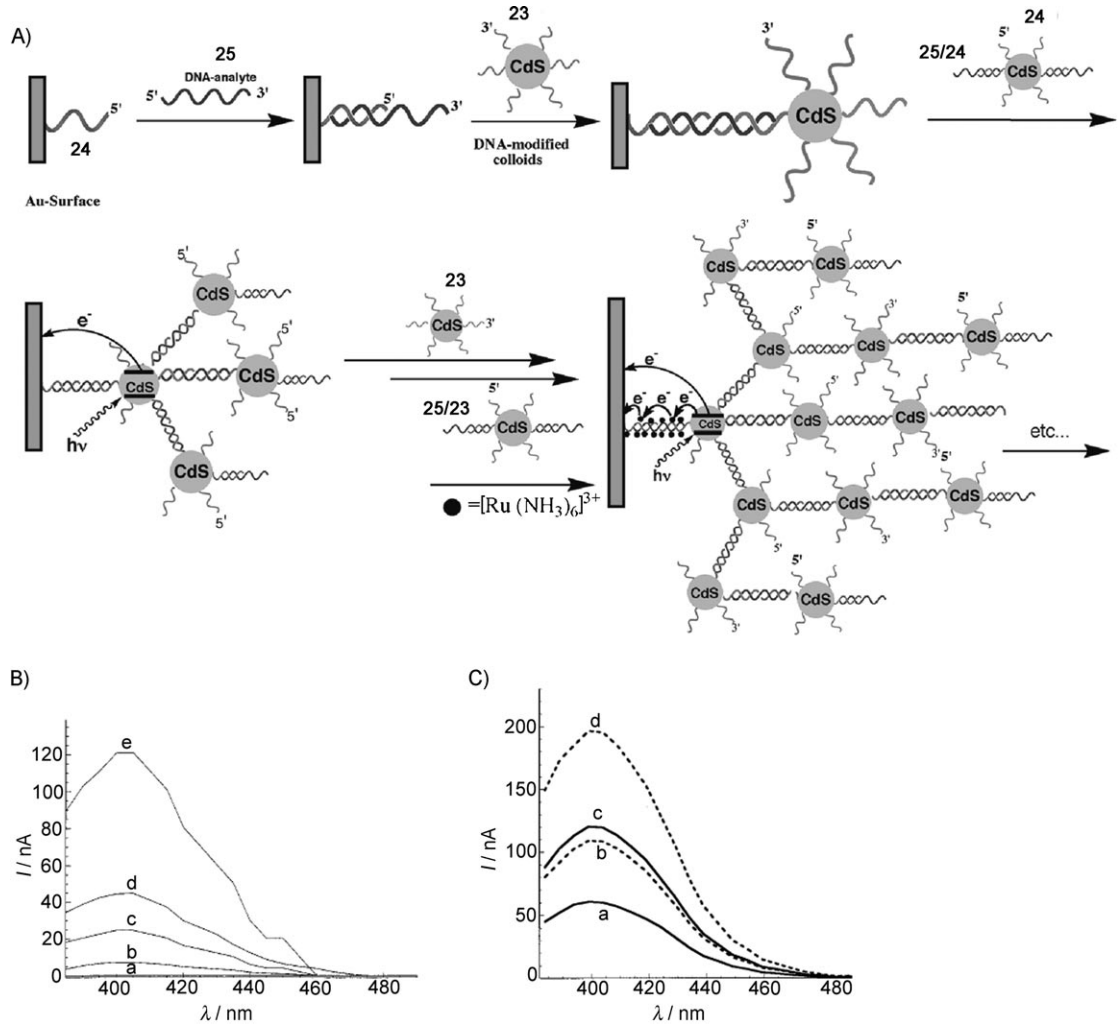

Figure 28. A) Layer-by-layer deposition of CdS NPs functionalized with **23** and **24** and crosslinked with **25**. The association of $[Ru(NH_3)_6]^{3+}$ to the DNA array facilitates charge transport and enhances the resulting photocurrent. B) Photocurrent action spectra generated by different numbers of CdS NP layers: a) no CdS NPs, b)–e) one to four layers. Photocurrents were recorded in the presence of triethanolamine (2×10^{-2} M). C) Effect of $[Ru(NH_3)_6]^{3+}$ (5×10^{-6} M) on the intensities of the photocurrents of layered CdS NP assemblies: a), b) two layers of CdS NP in the absence and presence of $[Ru(NH_3)_6]^{3+}$, respectively, c), d) four layers of CdS NP in the absence and presence of $[Ru(NH_3)_6]^{3+}$, respectively. Photocurrents were recorded in the presence of triethanolamine (2×10^{-2} M). (From Ref. [137]).

the DNA, enhanced the photocurrent from the DNA–CdS array. The $[Ru(NH_3)_6]^{3+}$ units acted as charge-transfer mediators that facilitated the hopping of conduction-band electrons from CdS particles, which lacked contact with the electrode owing to their separation by the DNA tethers (Figure 28C). The electrical contact of the photoexcited QDs with the electrode surface through the DNA bridging units is of fundamental interest.

Charge transport through DNA is a subject of scientific controversy, and whereas several studies claimed that DNA acts as a conducting matrix,[142] most results suggest that nucleic acids with a random distribution of bases behave as insulators.[143] The low photocurrents observed with semiconductor QDs separated by duplex nucleic acids from the electrode might support the insulating features of DNA, and suggest that the photocurrents originate from QD-nucleic acid hybrid structures in which the particles are in close contact with the electrode. The ability to intercalate redox-active components into duplex DNA may, however, provide a means to electrically contact the photoexcited semiconductor QDs with the electrode by charge transport through the intercalated units. Indeed, redox-active intercalators incorporated into double-strand DNAs that bridge semiconductor QDs to electrodes not only show enhanced photocurrent generation, but they enabled the potential-biased control of the photocurrent direction generated by the QDs.[138] The dithiolated single-strand DNA **26** was immobilized on gold surfaces and hybridized with the complementary dithiolated ssDNA **27**, which bridged the CdS nanoparticles to the surface (Figure 29A). The intercalation of doxorubicin (**28**) into the duplex DNA provided charge transfer relay units that enhanced the resulting photocurrent. A four-fold increase in the photocurrent intensity was observed relative to the system that lacked the intercalator units (Figure 29B).

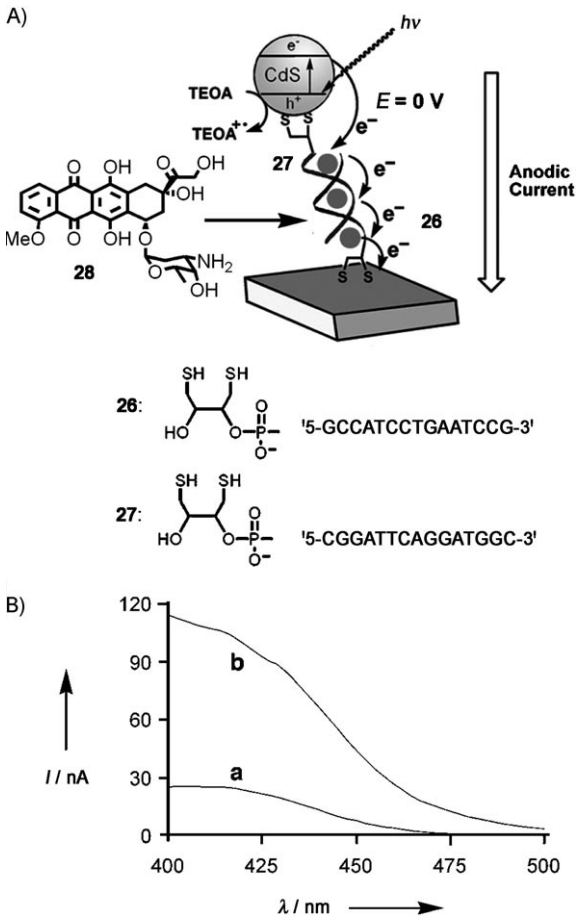

Figure 29. A) Photocurrent enhancement for CdS NPs linked to duplex DNA by the intercalation of doxorubicin **28** into the double-strand assembly. (B) Photocurrent action spectra for the CdS NPs/DNA duplex assembly a) without and b) with intercalator **28**. Photocurrents were recorded in the presence of triethanolamine (20 mM). (From Ref. [138]).

Self-assembly of CdS NPs on an electrode surface and photocurrent generation were employed as a readout method for the operation of a DNA machine (Figure 30A).[139] The system consisted of a DNA track **29** that included a recognition sequence (I), a nicking sequence generated upon the formation of a duplex structure (II), and a reporter sequence (III). Upon hybridization of **29** the analyte **30**, and in the presence of polymerase/dNTPs and the nicking enzyme Nb.BbvcI, the DNA machine was activated. This was reflected by the replication of the track and the subsequent scission of the resulting duplex. The nicking process initiated the further replication of the track and the displacement of the nucleic acid **31**. The displaced product **31** then interacted with an electrode modified with the nucleic acid **32**, complementary to the 3′ end of the product **31** and CdS NPs functionalized with the nucleic acid **33**, complementary to the 5′-end of the generated product **31**. This interaction resulted in the self-assembly of the CdS NPs on the electrode and the generation of a photocurrent (Figure 30B).

The formation of an electrical contact between semiconductor QDs and electrodes in the presence of proteins is more problematic because of the insulating features of proteins.[144] The tailored organization of semiconductor QD–protein hybrid assemblies on electrodes may, however, lead to electrically contacted architectures that are controlled by the linked proteins. In both configurations, the semiconductor QDs are directly linked to the electrode. The proteins are associated with the QD surface, and the control of the photoelectrochemical functions of the semiconductor QDs may then be accomplished by two general paths: 1) low-molecular-weight redox proteins might interact with the QDs, and the electrical contact between the conduction-band electrons/valence-band holes and the redox centers of the proteins might effect the photocurrents of the hybrid system; and 2) the biocatalyst may be tethered to the QDs, and their reaction products might act as electron-acceptor or electron-donor units, which may then activate the photoelectrochemical functions of the QDs.

Enzymes or redox-active proteins were linked to semiconductor QDs, and the resulting photocurrents were used to assay the enzyme activities and to develop further biosensors. Cytochrome c-mediated biocatalytic transformations were coupled to CdS NPs, and the direction of the resulting photocurrent was controlled by the oxidation-state of the cytochrome c mediator.[140] The CdS NPs were immobilized on a gold electrode by a dithiol linker, and mercaptopyridine

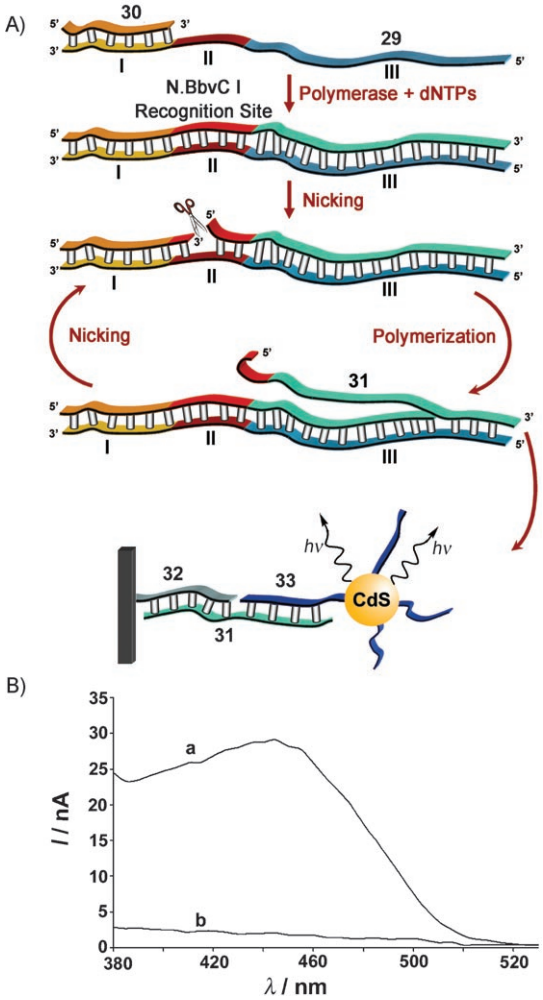

Figure 30. Photoelectrochemical readout of the sensing of a nucleic acid by a DNA machine. A) Amplified analysis of the target DNA **30** by a DNA machine that generates the sequence **31**. The association of the CdS NP functionalized with **33** on the electrode proceeds by bridging the NPs with the waste product **31**. B) Experimental photocurrents observed a) in the absence and b) in the presence of the target DNA (1×10^{-6} M). The DNA machine was operated for 90 min. Reproduced from Ref. [139] by permission of The Royal Society of Chemistry.

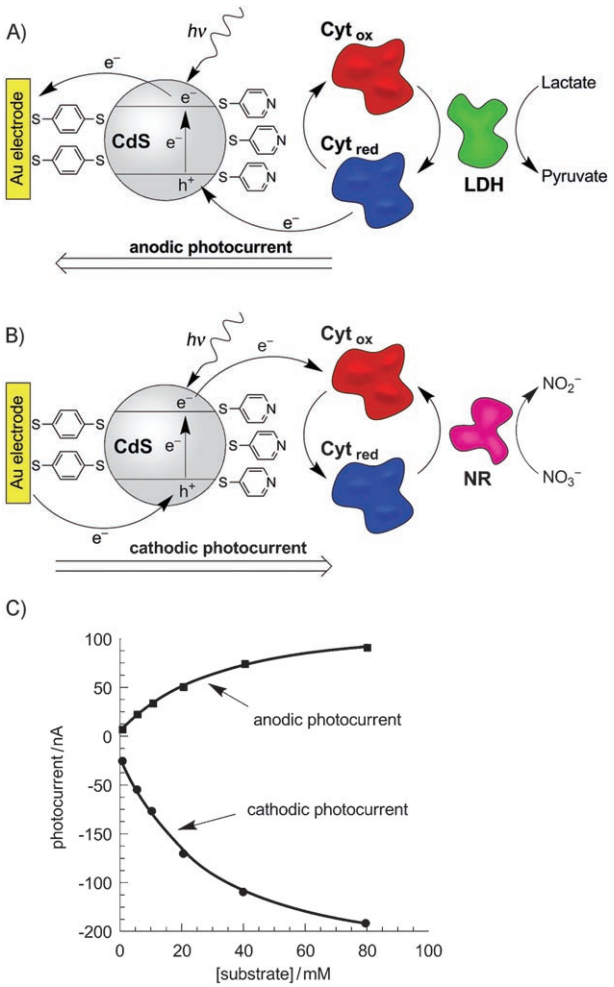

Figure 31. Generation of photocurrents by the photochemically induced activation of enzyme cascades by CdS NPs. Photochemical activation of the cytochrome c-mediated A) oxidation of lactate in the presence of LDH, and B) reduction of nitrate by nitrate reductase (NR). C) The photocurrents generated by the biocatalytic cascades in the presence of various concentrations of the substrates lactate and nitrate. Reproduced from Ref. [140] by permission of The Royal Society of Chemistry.

units, acting as promoter units that electrically communicate between the cytochrome c and the NPs, were linked to the semiconductor NPs (Figure 31). In the presence of reduced cytochrome c, the photoelectrocatalytic oxidation of lactate by lactate dehydrogenase (LDH) proceeded with the generation of an anodic photocurrent (Figure 31 A). Photoexcitation of the NPs resulted in the ejection of the conduction-band electrons into the electrode and the concomitant oxidation of the reduced cytochrome c by the valence-band holes. The resulting oxidized cytochrome c subsequently mediated the LDH-biocatalyzed oxidation of lactate. Similarly, cytochrome c in its oxidized form was used to stimulate the bioelectrocatalytic reduction of nitrate to nitrite in the presence of nitrate reductase (NR), generating a cathodic photocurrent (Figure 31 B). The transfer of conduction-band electrons to the oxidized cytochrome c was complemented by the transfer of electrons from the electrode to the valence-band holes of the NPs that restored the ground state of the NPs. The cytochrome c-mediated biocatalyzed reduction of nitrate to nitrite thus enabled the formation of the cathodic photocurrent when the electrode potential was biased at 0 V vs. SCE. The photocurrents generated by the biocatalytic cascades at various concentrations of the different substrates (Figure 31 C) show that the photoelectrochemical functions of semiconductor NPs could be used to develop sensors for biocatalytic transformations. A related study employed CdSe/ZnS QDs capped with mercaptosuccinic acid as the protecting layer for the generation of photocurrents in the presence of cytochrome c.[145]

The use of enzymes as catalysts which generate a product that stimulates the generation of a photocurrent by QDs was demonstrated by an acetylcholine esterase-based biosensor for the enzyme inhibitors.[141] CdS NPs were assembled on a gold electrode, and the NPs were further modified with

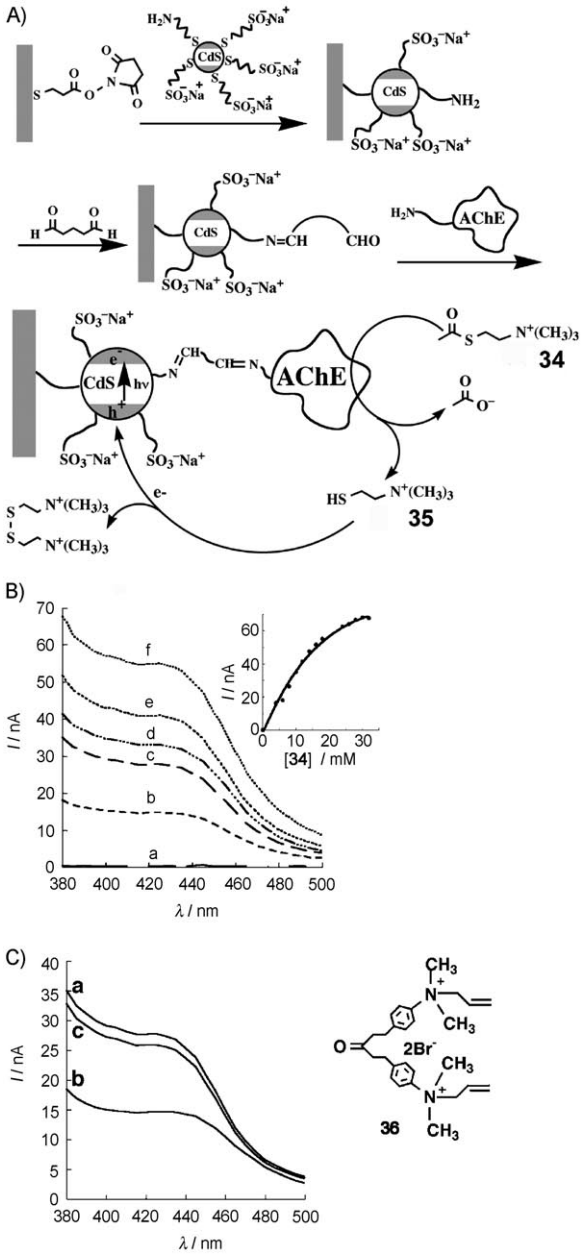

Figure 32. A) Assembly of a CdS NP/AChE hybrid system for the photoelectrochemical detection of the enzyme activity. B) Photocurrent action spectra observed in the presence of a) 0, b) 6, c) 10, d) 12, e) 16, and f) 30 mM acetylthiocholine **34**. Inset: Calibration curve of the photocurrent at $\lambda = 380$ nm at various concentrations of **34**. C) Photocurrent spectra for the CdS/AChE system in the presence of **34** (10 mM): a) in the absence of inhibitor **36**, b) upon addition of the inhibitor **36** (1×10^{-6} M), and c) after rinsing the system to remove the inhibitor, and addition of **34** (10 mM). Reprinted with permission from Ref. [141]. Copyright 2003 American Chemical Society.

acetylcholine esterase (AChE; Figure 32A). The biocatalyzed hydrolysis of acetylthiocholine **34** by acetylcholine esterase generated thiocholine **35**, which acted as an electron donor for the photogenerated holes in the valence band of the CdS NPs. The resulting photocurrents were controlled by the concentration of the substrate (Figure 32B), and the photocurrent intensities were depleted in the presence of inhibitors of acetylcholine esterase, such as 1,5-bis(4-allyldimethylammoniumphenyl)pentan-3-one dibromide **36** (Figure 32C). The system was suggested as a potential sensor for chemical warfare agents that act as inhibitors of acetylcholinesterase. Further photoelectrochemical detection of enzyme activity was demonstrated with the analysis of tyrosinase.[146] CdS nanoparticles functionalized with a thiolated tyrosine methyl ester **37** were reacted with tyrosinase/O_2, and the resulting dihydroxyphenyl methyl ester was linked to a phenylboronic acid monolayer-functionalized electrode (Figure 33A). The resulting photocurrent in the presence of triethanolamine (Figure 33B) was then used to analyze the enzyme activity. The detection limit for analysing tyrosinase was 0.2 U.

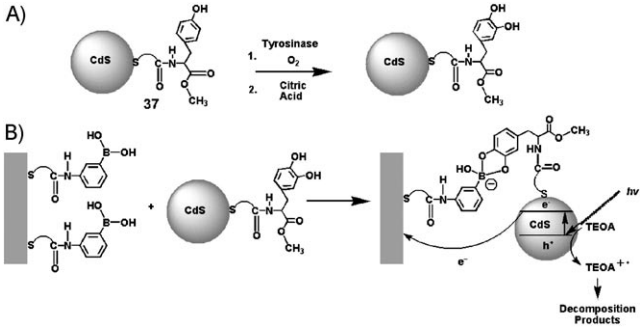

Figure 33. A) Tyrosinase/O_2-stimulated oxidation of CdS NPs functionalized with **37** to form the L-DOPA methyl ester product. B) Assembly of the L-DOPA methyl ester nanoparticles on a gold electrode for the generation of photocurrent. Reprinted in part with permission from Ref. [146]. Copyright 2008 American Chemical Society.

6. Semiconductor Nanoparticles as Electrochemical Labels for Biorecognition Events

The dimensions of semiconductor nanoparticles and their easy surface modification with biomolecules make them ideal high-surface-area, soluble, electrochemical tracers for biorecognition events. The subsequent chemical solubilization of the semiconductor nanoparticle labels, and the electrochemical stripping off of the released ions, provide quantitative readout signals for the labeled biomolecule analytes. This electrochemical sensing method is also useful in amplifying the recognition event, as numerous ions are released upon the dissolution of an individual NP.

Semiconductor NPs were employed as labels for the amplified electrochemical detection of proteins[147,148] and DNA.[149–151] The use of different semiconductor NPs enabled the parallel analysis of different targets, using the NPs as codes for different analytes. For example, CdS-semiconductor nanoparticles modified with nucleic acids were employed as labels for the detection of hybridization events of DNA.[152] Dissolution of the CdS in the presence of 1M nitric acid, followed by the electrochemical reduction of cadmium(II) to cadmium(0), resulted in accumulation of metal on the electrode. The subsequent stripping-off of the cadmium metal by oxidizing to cadmium(II) provided the electrical signal for the DNA analysis. This method was developed

further by using magnetic particles functionalized with nucleic acid probes as sensor units that hybridize with the analyte DNA, and nucleic acid-functionalized CdS NPs labels that hybridize with the single-strand domain of the analyte DNA and trace the primary formation of the probe/analyte double-strand complex. The magnetic separation of the magnetic particle/CdS NP aggregates crosslinked by the analyte DNA, followed by the dissolution of the CdS and electrochemical collection and stripping-off of the cadmium metal provide the amplified electrochemical readout of the analyte DNA. This system combines the advantages of magnetic separation of the trace amounts of CdS NPs associated with the DNA recognition events with the amplification features of the electrochemical stripping method. Highly sensitive detection of DNA is accomplished by this method (detection limit 100 fmol, reproducibility standard deviation 6%).[152]

Semiconductor NPs of various compositions can act as codes for the simultaneous and parallel analysis of different antibodies or DNAs. A model system for the multiplexed analysis of different nucleic acids with semiconductor NPs was developed (Figure 34A).[153] Three different kinds of magnetic particles were modified by three nucleic acids **38a–c**, and subsequently hybridized with the complementary target nucleic acids **39a–c**. The particles were then hybridized with three semiconductor nanoparticles (ZnS, CdS, and PbS), which were functionalized with nucleic acids **40a–c** complementary to the target nucleic acids associated with the magnetic particles. The magnetic particles allowed the easy separation and purification of the analyte samples, and the semiconductor particles provided non-overlapping electrochemical readout codes that transduced the specific kind of hybridized DNA. Stripping voltammetry of the respective semiconductor nanoparticles yielded well-defined and resolved stripping waves, which enabled the simultaneous electrochemical analysis of several DNA analytes. This method was further extended for coding unknown single nucleotide polymorphisms (SNPs) using different encoding QDs.[154] This procedure relies on the ZnS, CdS, PbS, and CuS NPs modified with four different mononucleotides and the application of the NPs to construct different combinations for specific SNPs that yielded a distinct electronic fingerprint for the mutation sites.

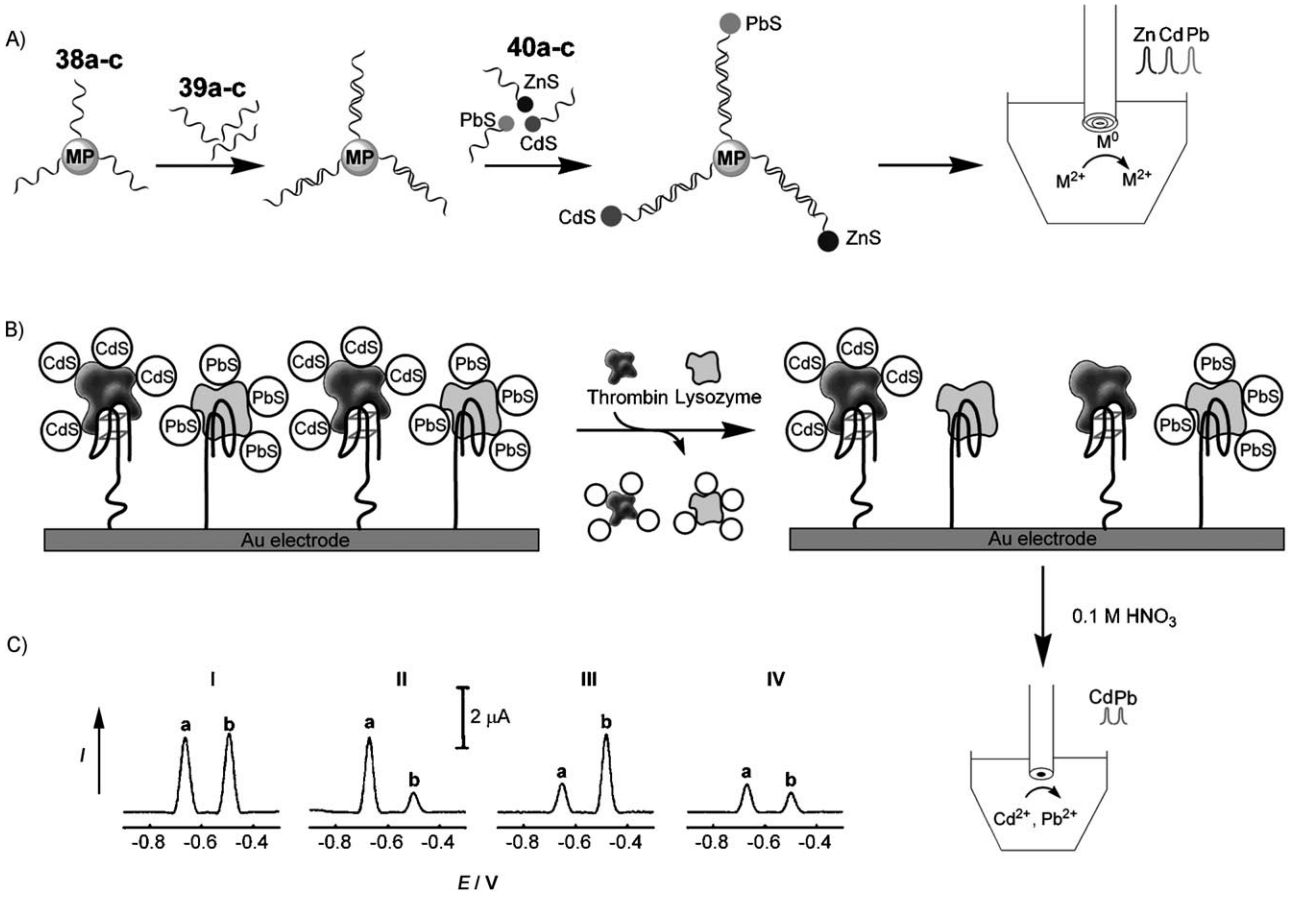

Figure 34. A) Parallel electrochemical analysis of different DNAs using magnetic particles functionalized with probes for the different DNA targets, and specific nucleic acid-functionalized metal sulfides as tracers. B) Simultaneous electrochemical analysis of the proteins thrombin and lysozyme using a competitive assay in which thrombin modified with CdS QDs and lysozyme modified with PbS QDs are used as tracers. C) Square-wave stripping voltammograms corresponding to the simultaneous detection of lysozyme (a) and thrombin (b): I) no (a) and no (b); II) 1 $\mu g\,L^{-1}$ (a), no (b); III) no (a), 0.5 $\mu g\,L^{-1}$ (b); IV) 1 $\mu g\,L^{-1}$ (a), 0.5 $\mu g\,L^{-1}$ (b). Reprinted in part with permission from Ref. [97]. Copyright 2006 American Chemical Society.

An analogous strategy was used for the multiplexed immunoassay of proteins[155] with simultaneous analysis of four different antigens. The arsenal of inorganic labels for the parallel multiplexed analysis of biomolecules and the level of amplification was further extended by using other metal sulfide composite nanostructures. For example, InS nanorods provided an additional resolvable voltammetric wave, and the nanorod configuration of the label increased the amplification efficiency owing to the higher content of stripped-off metal from the nanorod configuration relative to a spherical NP structure.[156]

This method to encode biomolecular identity by semiconductor NPs was extended to the parallel analysis of different proteins by their specific aptamers.[97] A gold electrode was functionalized with aptamers specific for thrombin and lysozyme (Figure 34B). Thrombin and lysozyme were labeled with CdS and PbS NPs, respectively, and the NP-functionalized proteins acted as tracer labels for analysis of the proteins. The competitive displacement of the respective labeled proteins associated with the surface by the analytes, followed by the dissolution of the metal sulfides associated with the surface and the detection of the released ions by electrochemical stripping, enabled then the quantitative detection of the two proteins (Figure 34C).

7. Conclusions and Perspectives

The unique photophysical properties and functions of semiconductor QDs have found growing interest in nanobiotechnology. The high fluorescence yields of QDs, their stability against photobleaching, and the size-controlled luminescence features of QDs has led to the development of different biosensing platforms. Apart from the advantages of using the QDs as effective luminescent labels, the multiplexed parallel analysis of targets by size-controlled luminescent QDs that act as coding labels shows great promise for future bioanalytical applications. The nanometer dimensions of QDs allows their incorporation into cells, and in vitro imaging of the QDs in different intracellular domains has already been demonstrated. The incorporation of functionalized QDs into cells to follow dynamic intracellular metabolic processes at the single-cell level also provides exciting future opportunities. The charge-ejection functions of semiconductor QDs hold also great promise for future nanomedical applications of QDs. The ejection of conduction-band electrons of semiconductor NPs into oxygen, and the formation of cell-destructive agents is well established,[157] and such particles have been suggested as cancer therapy materials. The successful incorporation of QDs into cells suggests that cell-targeted QDs could be synthesized and eventually act as tumor cell killers.

The use of biomolecule–QD hybrid systems for photoelectrochemical applications is still in its infancy, but the use of such hybrid structures for biosensing has been demonstrated. Future applications of these hybrid structures include the use of the hybrid structures as templates for the fabrication of devices. For example, DNA acts as a template for the synthesis of metallic nanowires by the reduction of metal ions linked to the DNA backbone.[158] The QD-stimulated photoelectrochemical reduction of ions associated with DNA may then lead to metal–semiconductor–metal nanostructured devices.

The extensive use of semiconductor QDs as light harvesting components for solar cells may benefit from biomolecule (specifically DNA)–semiconductor QD nanostructures.[137] The biomolecules may act as templates for metallic nanowires that trap the conduction-band electrons of the photoexcited QDs. This process could lead to enhanced charge separation and increased efficiencies of the resulting solar cells. The use of semiconductor nanoparticles as electrochemical tracers of biorecognition events are further possibilities for these nanostructures in bioanalysis. Nanoparticles of different composition provide a spectrum of labeling units that enable the multiplexed analysis of different targets, and together with the intrinsic amplification feature of the nanoparticles, adds a new dimension to their use in bioanalysis.

The rapid progress in tailoring functional biomolecule–semiconductor particle hybrid systems and their application in various bioanalytical applications indicates that the use of QDs goes beyond simple fluorescent labels. QDs as optical reporter units of biocatalytic transformations, their use for in vitro probing of intracellular processes, and the possibility of using the photoexited electron–hole pair for in vivo analysis and the stimulation of chemical transformations establish an exciting new field with bright perspectives for analysis, nanomedicine, and eventually, in vivo nanoelectronics.

Our research on biomolecule–semiconductor quantum dots is supported by the Israel Science Foundation, Converging Technologies Program and by the NanoSci-ERA consortium (NANOLICHT Project).

Received: January 13, 2008

[1] X. Wu, H. Liu, J. Liu, K. N. Haley, J. A. Treadway, J. P. Larson, N. Ge, F. Peale, M. P. Bruchez, *Nat. Biotechnol.* **2003**, *21*, 41–46.
[2] L. Brus, *Appl. Phys. A* **1991**, *53*, 465–474.
[3] A. P. Alivisatos, *Science* **1996**, *271*, 933–937.
[4] K. Grieve, P. Mulvaney, F. Grieser, *Curr. Opin. Colloid Interface Sci.* **2000**, *5*, 168–172.
[5] P. Alivisatos, *Nat. Biotechnol.* **2004**, *22*, 47–52.
[6] M. Nirmal, L. Brus, *Acc. Chem. Res.* **1999**, *32*, 407–414.
[7] Y. Xing, Q. Chaudry, C. Shen, K. Y. Kong, H. E. Zhau, L. W. Chung, J. A. Petros, R. M. O'Regan, M. V. Yezhelyev, J. W. Simons, M. D. Wang, S. Nie, *Nat. Protocols* **2007**, *2*, 1152–1165.
[8] I. Willner, B. Willner, E. Katz, *Bioelectrochemistry* **2007**, *70*, 2–11.
[9] R. Baron, B. Willner, I. Willner, *Chem. Commun.* **2007**, 323–332.
[10] P. V. Kamat, *J. Phys. Chem. C* **2007**, *111*, 2834–2860.
[11] T. Nakanishi, B. Ohtani, K. Uosaki, *J. Phys. Chem. B* **1998**, *102*, 1571–1577.
[12] L. Sheeney-Haj-Ichia, B. Basnar, I. Willner, *Angew. Chem.* **2005**, *117*, 80–85; *Angew. Chem. Int. Ed.* **2005**, *44*, 78–83.
[13] R. J. Ellingson, M. C. Beard, J. C. Johnson, P. R. Yu, O. I. Micic, A. J. Nozik, A. Shabaev, A. L. Efros, *Nano Lett.* **2005**, *5*, 865–871.

[14] R. D. Schaller, V. I. Klimov, *Phys. Rev. Lett.* **2004**, *92*, 186601.
[15] R. Plass, S. Pelet, J. Krueger, M. Gratzel, U. Bach, *J. Phys. Chem. B* **2002**, *106*, 7578 – 7580.
[16] A. J. Nozik, *Physica E* **2002**, *14*, 115 – 120.
[17] C. Y. Chen, C. T. Cheng, C. W. Lai, P. W. Wu, K. C. Wu, P. T. Chou, Y. H. Chou, H. T. Chiu, *Chem. Commun.* **2006**, 263 – 265.
[18] P. T. Snee, R. C. Somers, G. Nair, J. P. Zimmer, M. G. Bawendi, D. G. Nocera, *J. Am. Chem. Soc.* **2006**, *128*, 13320 – 13321.
[19] G. W. Walker, V. C. Sundar, C. M. Rudzinski, A. W. Wun, M. G. Bawendi, D. G. Nocera, *Appl. Phys. Lett.* **2003**, *83*, 3555 – 3557.
[20] I. L. Medintz, H. T. Uyeda, E. R. Goldman, H. Mattoussi, *Nat. Mater.* **2005**, *4*, 435 – 446.
[21] W. C. W. Chan, D. J. Maxwell, X. H. Gao, R. E. Bailey, M. Y. Han, S. M. Nie, *Curr. Opin. Biotechnol.* **2002**, *13*, 40 – 46.
[22] R. C. Somers, M. G. Bawendi, D. G. Nocera, *Chem. Soc. Rev.* **2007**, *36*, 579 – 591.
[23] S. R. Cordero, P. J. Carson, R. A. Estabrook, G. F. Strouse, S. K. Buratto, *J. Phys. Chem. B* **2000**, *104*, 12137 – 12142.
[24] H. Mattoussi, J. M. Mauro, E. R. Goldman, G. P. Anderson, V. C. Sundar, F. V. Mikulec, M. G. Bawendi, *J. Am. Chem. Soc.* **2000**, *122*, 12142 – 12150.
[25] W. C. W. Chan, S. M. Nie, *Science* **1998**, *281*, 2016 – 2018.
[26] D. Gerion, F. Pinaud, S. C. Williams, W. J. Parak, D. Zanchet, S. Weiss, A. P. Alivisatos, *J. Phys. Chem. B* **2001**, *105*, 8861 – 8871.
[27] M. Bruchez, Jr., M. Moronne, P. Gin, S. Weiss, A. P. Alivisatos, *Science* **1998**, *281*, 2013 – 2016.
[28] T. Pellegrino, L. Manna, S. Kudera, T. Liedl, D. Koktysh, A. L. Rogach, S. Keller, J. Raedler, G. Natile, W. J. Parak, *Nano Lett.* **2004**, *4*, 703 – 707.
[29] X. H. Gao, Y. Y. Cui, R. M. Levenson, L. W. K. Chung, S. M. Nie, *Nat. Biotechnol.* **2004**, *22*, 969 – 976.
[30] A. R. Clapp, I. L. Medintz, H. Mattoussi, *ChemPhysChem* **2006**, *7*, 47 – 57.
[31] K. E. Sapsford, L. Berti, I. L. Medintz, *Angew. Chem.* **2006**, *118*, 4676 – 4704; *Angew. Chem. Int. Ed.* **2006**, *45*, 4562 – 4588.
[32] A. M. Smith, H. W. Duan, M. N. Rhyner, G. Ruan, S. M. Nie, *Phys. Chem. Chem. Phys.* **2006**, *8*, 3895 – 3903.
[33] T. Pellegrino, S. Kudera, T. Liedl, A. M. Javier, L. Manna, W. J. Parak, *Small* **2005**, *1*, 48 – 63.
[34] M. Baumle, D. Stamou, J. M. Segura, R. Hovius, H. Vogel, *Langmuir* **2004**, *20*, 3828 – 3831.
[35] Y. G. Zheng, S. J. Gao, J. Y. Ying, *Adv. Mater.* **2007**, *19*, 376 – 380.
[36] K. Palaniappan, C. H. Xue, G. Arumugam, S. A. Hackney, J. Liu, *Chem. Mater.* **2006**, *18*, 1275 – 1280.
[37] D. M. Willard, L. L. Carillo, J. Jung, A. Van Orden, *Nano Lett.* **2001**, *1*, 469 – 474.
[38] S. P. Wang, N. Mamedova, N. A. Kotov, W. Chen, J. Studer, *Nano Lett.* **2002**, *2*, 817 – 822.
[39] I. L. Medintz, A. R. Clapp, H. Mattoussi, E. R. Goldman, B. Fisher, J. M. Mauro, *Nat. Mater.* **2003**, *2*, 630 – 638.
[40] H. T. Uyeda, I. L. Medintz, J. K. Jaiswal, S. M. Simon, H. Mattoussi, *J. Am. Chem. Soc.* **2005**, *127*, 3870 – 3878.
[41] W. Liu, M. Howarth, A. B. Greytak, Y. Zheng, D. G. Nocera, A. Y. Ting, M. G. Bawendi, *J. Am. Chem. Soc.* **2008**, *130*, 1274 – 1284.
[42] F. Pinaud, D. King, H. P. Moore, S. Weiss, *J. Am. Chem. Soc.* **2004**, *126*, 6115 – 6123.
[43] G. Iyer, F. Pinaud, J. Tsay, S. Weiss, *Small* **2007**, *3*, 793 – 798.
[44] Y. Liu, R. Brandon, M. Cate, X. Peng, R. Stony, M. Johnson, *Anal. Chem.* **2007**, *79*, 8796 – 8802.
[45] Y. C. Liu, M. Kim, Y. J. Wang, Y. A. Wang, X. G. Peng, *Langmuir* **2006**, *22*, 6341 – 6345.
[46] W. W. Yu, E. Chang, J. C. Falkner, J. Y. Zhang, A. M. Al-Somali, C. M. Sayes, J. Johns, R. Drezek, V. L. Colvin, *J. Am. Chem. Soc.* **2007**, *129*, 2871 – 2879.
[47] M. S. Nikolic, M. Krack, V. Aleksandrovic, A. Kornowski, S. Förster, H. Weller, *Angew. Chem.* **2006**, *118*, 6727 – 6731; *Angew. Chem. Int. Ed.* **2006**, *45*, 6577 – 6580.
[48] D. J. Zhou, J. D. Piper, C. Abell, D. Klenerman, D. J. Kang, L. M. Ying, *Chem. Commun.* **2005**, 4807 – 4809.
[49] E. R. Goldman, E. D. Balighian, H. Mattoussi, M. K. Kuno, J. M. Mauro, P. T. Tran, G. P. Anderson, *J. Am. Chem. Soc.* **2002**, *124*, 6378 – 6382.
[50] Z. B. Lin, S. X. Cui, H. Zhang, Q. D. Chen, B. Yang, X. G. Su, J. H. Zhang, Q. H. Jin, *Anal. Biochem.* **2003**, *319*, 239 – 243.
[51] S. Pathak, M. C. Davidson, G. A. Silva, *Nano Lett.* **2007**, *7*, 1839 – 1845.
[52] E. R. Goldman, I. L. Medintz, A. Hayhurst, G. P. Anderson, J. M. Mauro, B. L. Iverson, G. Georgiou, H. Mattoussi, *Anal. Chim. Acta* **2005**, *534*, 63 – 67.
[53] U. L. Lao, A. Mulchandani, W. Chen, *J. Am. Chem. Soc.* **2006**, *128*, 14756 – 14757.
[54] I. L. Medintz, A. R. Clapp, F. M. Brunel, T. Tiefenbrunn, H. T. Uyeda, E. L. Chang, J. R. Deschamps, P. E. Dawson, H. Mattoussi, *Nat. Mater.* **2006**, *5*, 581 – 589.
[55] I. L. Medintz, L. Berti, T. Pons, A. F. Grimes, D. S. English, A. Alessandrini, P. Facci, H. Mattoussi, *Nano Lett.* **2007**, *7*, 1741 – 1748.
[56] M. Miyake, H. Matsumoto, M. Nishizawa, T. Sakata, H. Mori, S. Kuwabata, H. Yoneyama, *Langmuir* **1997**, *13*, 742 – 746.
[57] E. Granot, F. Patolsky, I. Willner, *J. Phys. Chem. B* **2004**, *108*, 5875 – 5881.
[58] P. J. Cameron, X. Zhong, W. Knoll, *J. Phys. Chem. C* **2007**, *111*, 10313 – 10319.
[59] R. Baron, C. H. Huang, D. M. Bassani, A. Onopriyenko, M. Zayats, I. Willner, *Angew. Chem.* **2005**, *117*, 4078 – 4083; *Angew. Chem. Int. Ed.* **2005**, *44*, 4010 – 4015.
[60] K. E. Sapsford, T. Pons, I. L. Medintz, H. Mattoussi, *Sensors* **2006**, *6*, 925 – 953.
[61] J. M. Costa-Fernandez, R. Pereiro, A. Sanz-Medel, *TrAC Trends Anal. Chem.* **2006**, *25*, 207 – 218.
[62] J. M. Klostranec, W. C. W. Chan, *Adv. Mater.* **2006**, *18*, 1953 – 1964.
[63] C. J. Murphy, *Anal. Chem.* **2002**, *74*, 520A – 526A.
[64] M. Shingyoji, D. Gerion, D. Pinkel, J. W. Gray, F. Q. Chen, *Talanta* **2005**, *67*, 472 – 478.
[65] A. Zajac, D. S. Song, W. Qian, T. Zhukov, *Colloids Surf. B* **2007**, *58*, 309 – 314.
[66] E. R. Goldman, G. P. Anderson, P. T. Tran, H. Mattoussi, P. T. Charles, J. M. Mauro, *Anal. Chem.* **2002**, *74*, 841 – 847.
[67] E. R. Goldman, A. R. Clapp, G. P. Anderson, H. T. Uyeda, J. M. Mauro, I. L. Medintz, H. Mattoussi, *Anal. Chem.* **2004**, *76*, 684 – 688.
[68] L. J. Yang, Y. B. Li, *Analyst* **2006**, *131*, 394 – 401.
[69] A. Hoshino, K. Fujioka, N. Manabe, S. Yamaya, Y. Goto, M. Yasuhara, K. Yamamoto, *Microbiol. Immunol.* **2005**, *49*, 461 – 470.
[70] D. Gerion, F. Q. Chen, B. Kannan, A. H. Fu, W. J. Parak, D. J. Chen, A. Majumdar, A. P. Alivisatos, *Anal. Chem.* **2003**, *75*, 4766 – 4772.
[71] R. Q. Liang, W. Li, Y. Li, C. Y. Tan, J. X. Li, Y. X. Jin, K. C. Ruan, *Nucleic Acids Res.* **2005**, *33*, e17.
[72] R. Bakalova, Z. Zhelev, H. Ohba, Y. Baba, *J. Am. Chem. Soc.* **2005**, *127*, 11328 – 11335.
[73] S. Pathak, S. K. Choi, N. Arnheim, M. E. Thompson, *J. Am. Chem. Soc.* **2001**, *123*, 4103 – 4104.
[74] Y. Xiao, P. E. Barker, *Nucleic Acids Res.* **2004**, *32*, e28.
[75] P. M. Chan, T. Yuen, F. Ruf, J. Gonzalez-Maeso, S. C. Sealfon, *Nucleic Acids Res.* **2005**, *33*, e161.
[76] S. M. Wu, X. Zha, Z. L. Zhang, H. Y. Xie, Z. Q. Tian, J. Peng, Z. X. Lu, D. W. Pang, Z. X. Xie, *ChemPhysChem* **2006**, *7*, 1062 – 1067.

[77] P. S. Eastman, W. M. Ruan, M. Doctolero, R. Nuttall, G. De Feo, J. S. Park, J. S. F. Chu, P. Cooke, J. W. Gray, S. Li, F. Q. F. Chen, *Nano Lett.* **2006**, *6*, 1059 – 1064.
[78] M. Y. Han, X. H. Gao, J. Z. Su, S. Nie, *Nat. Biotechnol.* **2001**, *19*, 631 – 635.
[79] J. M. Klostranec, Q. Xiang, G. A. Farcas, J. A. Lee, A. Rhee, E. I. Lafferty, S. D. Perrault, K. C. Kain, W. C. W. Chan, *Nano Lett.* **2007**, *7*, 2812 – 2818.
[80] A. Sukhanova, A. S. Susha, A. Bek, S. Mayilo, A. L. Rogach, J. Feldmann, V. Oleinikov, B. Reveil, B. Donvito, J. H. M. Cohen, I. Nabiev, *Nano Lett.* **2007**, *7*, 2322 – 2327.
[81] I. Yildiz, M. Tomasulo, F. M. Raymo, *Proc. Natl. Acad. Sci. USA* **2006**, *103*, 11457 – 11460.
[82] E. R. Goldman, I. L. Medintz, J. L. Whitley, A. Hayhurst, A. R. Clapp, H. T. Uyeda, J. R. Deschamps, M. E. Lassman, H. Mattoussi, *J. Am. Chem. Soc.* **2005**, *127*, 6744 – 6751.
[83] E. Oh, D. Lee, Y. P. Kim, S. Y. Cha, D. B. Oh, H. A. Kang, J. Kim, H. S. Kim, *Angew. Chem.* **2006**, *118*, 8127 – 8131; *Angew. Chem. Int. Ed.* **2006**, *45*, 7959 – 7963.
[84] I. L. Medintz, A. R. Clapp, J. S. Melinger, J. R. Deschamps, H. Mattoussi, *Adv. Mater.* **2005**, *17*, 2450 – 2455.
[85] L. F. Shi, V. De Paoli, N. Rosenzweig, Z. Rosenzweig, *J. Am. Chem. Soc.* **2006**, *128*, 10378 – 10379.
[86] E. Chang, J. S. Miller, J. T. Sun, W. W. Yu, V. L. Colvin, R. Drezek, J. L. West, *Biochem. Biophys. Res. Commun.* **2005**, *334*, 1317 – 1321.
[87] L. F. Shi, N. Rosenzweig, Z. Rosenzweig, *Anal. Chem.* **2007**, *79*, 208 – 214.
[88] F. Patolsky, R. Gill, Y. Weizmann, T. Mokari, U. Banin, I. Willner, *J. Am. Chem. Soc.* **2003**, *125*, 13918 – 13919.
[89] R. K. Moyzis, J. M. Buckingham, L. S. Cram, M. Dani, L. L. Deaven, M. D. Jones, J. Meyne, R. L. Ratliff, J. R. Wu, *Proc. Natl. Acad. Sci. USA* **1988**, *85*, 6622 – 6626.
[90] T. M. Bryan, T. R. Cech, *Curr. Opin. Cell Biol.* **1999**, *11*, 318 – 324.
[91] N. W. Kim, M. A. Piatyszek, K. R. Prowse, C. B. Harley, M. D. West, P. L. C. Ho, G. M. Coviello, W. E. Wright, S. L. Weinrich, J. W. Shay, *Science* **1994**, *266*, 2011 – 2015.
[92] J. W. Shay, S. Bacchetti, *Eur. J. Cancer* **1997**, *33*, 787 – 791.
[93] J. H. Kim, D. Morikis, M. Ozkan, *Sens. Actuators B* **2004**, *102*, 315 – 319.
[94] J. H. Kim, S. Chaudhary, M. Ozkan, *Nanotechnology* **2007**, *18*, 195105.
[95] N. C. Cady, A. D. Strickland, C. A. Batt, *Mol. Cell. Probes* **2007**, *21*, 116 – 124.
[96] R. Gill, I. Willner, I. Shweky, U. Banin, *J. Phys. Chem. B* **2005**, *109*, 23715 – 23719.
[97] J. A. Hansen, J. Wang, A. N. Kawde, Y. Xiang, K. V. Gothelf, G. Collins, *J. Am. Chem. Soc.* **2006**, *128*, 2228 – 2229.
[98] R. Polsky, R. Gill, L. Kaganovsky, I. Willner, *Anal. Chem.* **2006**, *78*, 2268 – 2271.
[99] V. Pavlov, Y. Xiao, B. Shlyahovsky, I. Willner, *J. Am. Chem. Soc.* **2004**, *126*, 11768 – 11769.
[100] J. Liu, Y. Lu, *Angew. Chem.* **2006**, *118*, 96 – 100; *Angew. Chem. Int. Ed.* **2006**, *45*, 90 – 94.
[101] M. Levy, S. F. Cater, A. D. Ellington, *ChemBioChem* **2005**, *6*, 2163 – 2166.
[102] J. H. Choi, K. H. Chen, M. S. Strano, *J. Am. Chem. Soc.* **2006**, *128*, 15584 – 15585.
[103] J. W. Liu, J. H. Lee, Y. Lu, *Anal. Chem.* **2007**, *79*, 4120 – 4125.
[104] Z. Gueroui, A. Libchaber, *Phys. Rev. Lett.* **2004**, *93*, 166108.
[105] S. Hohng, T. Ha, *ChemPhysChem* **2005**, *6*, 956 – 960.
[106] Y. P. Ho, M. C. Kung, S. Yang, T. H. Wang, *Nano Lett.* **2005**, *5*, 1693 – 1697.
[107] H. C. Yeh, Y. P. Ho, I. M. Shih, T. H. Wang, *Nucleic Acids Res.* **2006**, *34*, e35.
[108] A. Agrawal, C. Y. Zhang, T. Byassee, R. A. Tripp, S. M. Nie, *Anal. Chem.* **2006**, *78*, 1061 – 1070.
[109] C. Y. Zhang, H. C. Yeh, M. T. Kuroki, T. H. Wang, *Nat. Mater.* **2005**, *4*, 826 – 831.
[110] T. Pons, I. L. Medintz, X. Wang, D. S. English, H. Mattoussi, *J. Am. Chem. Soc.* **2006**, *128*, 15324 – 15331.
[111] C. Y. Zhang, L. W. Johnson, *Angew. Chem.* **2007**, *119*, 3552 – 3555; *Angew. Chem. Int. Ed.* **2007**, *46*, 3482 – 3485.
[112] C. Y. Zhang, L. W. Johnson, *Anal. Chem.* **2007**, *79*, 7775 – 7781.
[113] A. R. Clapp, I. L. Medintz, B. R. Fisher, G. P. Anderson, H. Mattoussi, *J. Am. Chem. Soc.* **2005**, *127*, 1242 – 1250.
[114] N. Hildebrandt, L. J. Charbonnière, M. Beck, R. F. Ziessel, H.-G. Löhmannsröben, *Angew. Chem.* **2005**, *117*, 7784 – 7788; *Angew. Chem. Int. Ed.* **2005**, *44*, 7612 – 7615.
[115] L. J. Charbonnière, N. Hildebrandt, R. F. Ziessel, H.-G. Löhmannsröben, *J. Am. Chem. Soc.* **2006**, *128*, 12800 – 12809.
[116] M. K. So, C. J. Xu, A. M. Loening, S. S. Gambhir, J. H. Rao, *Nat. Biotechnol.* **2006**, *24*, 339 – 343.
[117] H. Q. Yao, Y. Zhang, F. Xiao, Z. Y. Xia, J. H. Rao, *Angew. Chem.* **2007**, *119*, 4424 – 4427; *Angew. Chem. Int. Ed.* **2007**, *46*, 4346 – 4349.
[118] M. G. Sandros, D. Gao, D. E. Benson, *J. Am. Chem. Soc.* **2005**, *127*, 12198 – 12199.
[119] B. P. Aryal, D. E. Benson, *J. Am. Chem. Soc.* **2006**, *128*, 15986 – 15987.
[120] R. Gill, R. Freeman, J. P. Xu, I. Willner, S. Winograd, I. Shweky, U. Banin, *J. Am. Chem. Soc.* **2006**, *128*, 15376 – 15377.
[121] R. Gill, L. Bahshi, R. Freeman, I. Willner, *Angew. Chem.* **2008**, *120*, 1700 – 1703; *Angew. Chem. Int. Ed.* **2008**, *47*, 1676 – 1679.
[122] A. Roda, P. Pasini, M. Guardigli, M. Baraldini, M. Musiani, M. Mirasoli, *Fresenius J. Anal. Chem.* **2000**, *366*, 752 – 759.
[123] W. Y. Lee, *Mikrochim. Acta* **1997**, *127*, 19 – 39.
[124] F. Patolsky, Y. Weizmann, E. Katz, I. Willner, *Angew. Chem.* **2003**, *115*, 2474 – 2478; *Angew. Chem. Int. Ed.* **2003**, *42*, 2372 – 2376.
[125] C. Dodeigne, L. Thunus, R. Lejeune, *Talanta* **2000**, *51*, 415 – 439.
[126] V. Pavlov, Y. Xiao, R. Gill, A. Dishon, M. Kotler, I. Willner, *Anal. Chem.* **2004**, *76*, 2152 – 2156.
[127] Y. Weizmann, M. K. Beissenhirtz, Z. Cheglakov, R. Nowarski, M. Kotler, I. Willner, *Angew. Chem.* **2006**, *118*, 7544 – 7548; *Angew. Chem. Int. Ed.* **2006**, *45*, 7384 – 7388.
[128] J. Rodriguez-Viejo, K. F. Jensen, H. Mattoussi, J. Michel, B. O. Dabbousi, M. G. Bawendi, *Appl. Phys. Lett.* **1997**, *70*, 2132 – 2134.
[129] S. K. Poznyak, D. V. Talapin, E. V. Shevchenko, H. Weller, *Nano Lett.* **2004**, *4*, 693 – 698.
[130] N. Myung, Z. F. Ding, A. J. Bard, *Nano Lett.* **2002**, *2*, 1315 – 1319.
[131] G. Z. Zou, H. X. Ju, *Anal. Chem.* **2004**, *76*, 6871 – 6876.
[132] H. Y. Han, Z. G. Sheng, J. G. Liang, *Anal. Chim. Acta* **2007**, *596*, 73 – 78.
[133] H. Jiang, H. X. Ju, *Anal. Chem.* **2007**, *79*, 6690 – 6696.
[134] H. Jiang, H. X. Ju, *Chem. Commun.* **2007**, 404 – 406.
[135] X. Liu, H. Jiang, J. P. Lei, H. X. Ju, *Anal. Chem.* **2007**, *79*, 8055 – 8060.
[136] Y. X. Li, P. Yang, P. Wang, X. Huang, L. Wang, *Nanotechnology* **2007**, *18*, 225602.
[137] I. Willner, F. Patolsky, J. Wasserman, *Angew. Chem.* **2001**, *113*, 1913 – 1916; *Angew. Chem. Int. Ed.* **2001**, *40*, 1861 – 1864.
[138] R. Gill, F. Patolsky, E. Katz, I. Willner, *Angew. Chem.* **2005**, *117*, 4630 – 4633; *Angew. Chem. Int. Ed.* **2005**, *44*, 4554 – 4557.
[139] R. Freeman, R. Gill, M. Beissenhirtz, I. Willner, *Photochem. Photobiol. Sci.* **2007**, *6*, 416 – 422.
[140] E. Katz, M. Zayats, I. Willner, F. Lisdat, *Chem. Commun.* **2006**, 1395 – 1397.
[141] V. Pardo-Yissar, E. Katz, J. Wasserman, I. Willner, *J. Am. Chem. Soc.* **2003**, *125*, 622 – 623.

[142] D. Porath, G. Cuniberti, R. Di Felice, *Top. Curr. Chem.* **2004**, *237*, 183 – 227.
[143] P. J. de Pablo, F. Moreno-Herrero, J. Colchero, J. Gomez-Herrero, P. Herrero, A. M. Baro, P. Ordejon, J. M. Soler, E. Artacho, *Phys. Rev. Lett.* **2000**, *85*, 4992 – 4995.
[144] I. Willner, *Science* **2002**, *298*, 2407 – 2408.
[145] C. Stoll, S. Kudera, W. J. Parak, F. Lisdat, *Small* **2006**, *2*, 741 – 743.
[146] H. B. Yildiz, R. Freeman, R. Gill, B. Willner, *Anal. Chem.* **2008**, *80*, 2811 – 2816.
[147] H. Wu, G. D. Liu, J. Wang, Y. H. Lin, *Electrochem. Commun.* **2007**, *9*, 1573 – 1577.
[148] G. Liu, Y. Y. Lin, J. Wang, H. Wu, C. M. Wai, Y. Lin, *Anal. Chem.* **2007**, *79*, 7644 – 7653.
[149] J. Wang, *Small* **2005**, *1*, 1036 – 1043.
[150] A. Merkoci, M. Aldavert, S. Marin, S. Alegret, *TrAC Trends Anal. Chem.* **2005**, *24*, 341 – 349.
[151] A. Merkoci, *FEBS J.* **2007**, *274*, 310 – 316.
[152] J. Wang, G. D. Liu, R. Polsky, A. Merkoci, *Electrochem. Commun.* **2002**, *4*, 722 – 726.
[153] J. Wang, G. D. Liu, A. Merkoci, *J. Am. Chem. Soc.* **2003**, *125*, 3214 – 3215.
[154] G. Liu, T. M. H. Lee, J. Wang, *J. Am. Chem. Soc.* **2005**, *127*, 38 – 39.
[155] G. D. Liu, J. Wang, J. Kim, M. R. Jan, G. E. Collins, *Anal. Chem.* **2004**, *76*, 7126 – 7130.
[156] J. Wang, G. D. Liu, Q. Y. Zhu, *Anal. Chem.* **2003**, *75*, 6218 – 6222.
[157] R. Bakalova, H. Ohba, Z. Zhelev, M. Ishikawa, Y. Baba, *Nat. Biotechnol.* **2004**, *22*, 1360 – 1361.
[158] E. Braun, Y. Eichen, U. Sivan, G. Ben-Yoseph, *Nature* **1998**, *391*, 775 – 778.

